



HAL
open science

Synergistic effects of temperature and light affect the relationship between *Taonia atomaria* and its epibacterial community: a controlled conditions study

Benoit Paix, Philippe Potin, Gaëtan Schires, Christophe Le Poupon, B. Misson, Catherine Leblanc, Gérald Culioli, Jean-françois Briand

► To cite this version:

Benoit Paix, Philippe Potin, Gaëtan Schires, Christophe Le Poupon, B. Misson, et al.. Synergistic effects of temperature and light affect the relationship between *Taonia atomaria* and its epibacterial community: a controlled conditions study. *Environmental Microbiology*, 2021, 23 (11), pp.6777-6797. 10.1111/1462-2920.15758 . hal-03400714

HAL Id: hal-03400714

<https://amu.hal.science/hal-03400714>

Submitted on 16 Mar 2022

HAL is a multi-disciplinary open access archive for the deposit and dissemination of scientific research documents, whether they are published or not. The documents may come from teaching and research institutions in France or abroad, or from public or private research centers.

L'archive ouverte pluridisciplinaire **HAL**, est destinée au dépôt et à la diffusion de documents scientifiques de niveau recherche, publiés ou non, émanant des établissements d'enseignement et de recherche français ou étrangers, des laboratoires publics ou privés.

1 Synergistic effects of temperature and light affect the relationship
2 between *Taonia atomaria* and its epibacterial community:
3 a controlled conditions study
4

5 Benoit Paix^{a,1}, Philippe Potin^b, Gaëtan Schires^c, Christophe Le Poupon^d, Benjamin Misson^d,
6 Catherine Leblanc^b, Gérald Culioli^{a,2,*} and Jean-François Briand^{a,*}

7
8 ^a*Université de Toulon, Laboratoire MAPIEM, EA 4323, La Garde, France*

9 ^b*Sorbonne Université, CNRS, Integrative Biology of Marine Models (LBI2M), UMR 8227, Station*
10 *Biologique de Roscoff (SBR), Roscoff, France*

11 ^c*Sorbonne Université, CNRS, Center for Biological Marine Ressources (CRBM), FR 2424, Station*
12 *Biologique de Roscoff (SBR), Roscoff, France*

13 ^d*Université de Toulon, Aix Marseille Université, CNRS, IRD, Mediterranean Institute of*
14 *Oceanography (MIO), UM110, La Garde, France*

15
16 *corresponding authors: briand@univ-tln.fr, gerald.culioli@univ-avignon.fr

17 **Running head:** Temperature and light affect holobiont dynamics

18
19 ¹ New affiliation: *Marine Biodiversity, Naturalis Biodiversity Center, Leiden, The Netherlands.*

20 ² New affiliation: *Institut Méditerranéen de Biodiversité et d'Ecologie marine et continentale*
21 *(IMBE), UMR CNRS-IRD-Avignon Université-Aix-Marseille Université, Avignon, France.*

23 Originality-Significance Statement

24 We developed an experimental set up using controlled conditions, supplied by natural seawater,
25 to test an algal holobiont response to changes of temperature combined with those of irradiance
26 over 14 days, and using a multi-omics approach coupling algal surface metabolomics and
27 metabarcoding.

28

29

30 Summary

31 In a context of global warming, this study aimed to assess the effect of temperature and irradiance
32 on the macroalgal *Taonia atomaria* holobiont dynamics. We developed an experimental set up
33 using aquaria supplied by natural seawater with three temperatures combined with three
34 irradiances. The holobiont response was monitored over 14 days using a multi-omics approach
35 coupling algal surface metabolomics and metabarcoding. Both temperature and irradiance
36 appeared to shape the microbiota and the surface metabolome, but with a distinct temporality.
37 Epibacterial community firstly changed according to temperature, and later in relation to
38 irradiance, while the opposite occurred for the surface metabolome. An increased temperature
39 revealed a decreasing richness of the epiphytic community together with an increase of several
40 bacterial taxa. Irradiance changes appeared to quickly impact surface metabolites production
41 linked with the algal host photosynthesis (e.g. mannitol, fucoxanthin, DMSP), which was
42 hypothesized to explain modifications of the structure of the epiphytic community. Algal host
43 may also directly adapt its surface metabolome to changing temperature with time (e.g. lipids
44 content) but also in response to changing microbiota (e.g. chemical defenses). Finally, this study
45 brought new insights highlighting complex direct and indirect responses of seaweeds and their
46 associated microbiota under changing environments.

47

48 Keywords: holobiont, surface metabolome, surface microbiota, metabolomics, controlled
49 condition experiments, multi-omics

50

51 Introduction

52 As marine holobionts, macroalgae are known to establish intimate relationships with their
53 epiphytic microbiota (Hollants et al., 2013). Notably, macroalgae are capable of controlling their
54 epibacterial consortia through chemical defenses as well as chemoattractants released at their
55 surface (Harder et al., 2012; Wahl et al., 2012; Wichard et al., 2015). Such negative or positive
56 chemical mediations play an important role for the host physiology and, for example, can be
57 associated to immune or development processes (Wichard and Beemelmans, 2018). As sessile
58 organisms in intertidal and infralittoral zones, marine macroalgae are subject to many
59 environmental changes often linked to anthropogenic stresses, such as global warming or marine
60 coastal pollution (Dittami et al., 2014; van der Loos et al., 2019). Concerns are notably raised to
61 understand how climate changes will drive seaweed-bacteria interactions in the future (Campbell
62 et al., 2011; Egan et al., 2014; Egan and Gardiner, 2016). As for other marine holobionts such as
63 corals and sponges, temperature increase and seawater acidification are the most investigated
64 factors for macroalgae in this context of global changes (van der Loos et al., 2019).

65 Among macroalgae, the bleaching disease of the Rhodophyta *Delisea pulchra* has been directly
66 correlated to the temperature increase. This alga produces chemical defenses, identified as
67 halogenated furanones, known to act as quorum sensing inhibitors and protecting the seaweed
68 against bleaching disease (Maximilien et al., 1998; Harder et al., 2012). However, algae that
69 bleach in response to water temperature increases, features lower levels of these defenses
70 (Campbell et al., 2011; Case et al., 2011). In these specific conditions, several opportunistic
71 bacteria (e.g. *Nautella italica* and *Phaeobacter* sp.) are observed at the algal surface and have
72 been proposed to be involved in the bleaching phenomenon (Case et al., 2011; Fernandes et al.,
73 2011; Campbell et al., 2014; Kumar et al., 2016). Even if temperature alone failed to explain the
74 bleaching disease (Zozaya-Valdés et al., 2016), a global decrease of macroalgal health and
75 dysbiosis should be a plausible scenario to anticipate in the context of global warming (Egan et
76 al., 2014).

77 In the last few years, the combined effect of the rise of temperature and seawater acidification
78 on macroalgal physiology and surface microbiota has been increasingly studied through
79 controlled conditions experiments. While for the Chlorophyta *Caulerpa taxifolia* mitigating effects

80 are observed (Roth-Schulze et al., 2018), predicted future climate conditions influence the
81 microbiota structure for the Phaeophyceae *Eklonia radiata* (Qiu et al., 2019), *Macrocystis pyrifera*
82 (Minich et al., 2018), *Fucus vesiculosus forma mytili* (Mensch et al., 2016) and the Rhodophyta
83 *Amphiroa gracilis* (Huggett et al., 2018). Moreover, the host physiology is also disturbed with
84 blistered tissues and reduced photosynthetic efficiency for *E. radiata*, bleaching disease for *A.*
85 *gracilis* and growth reduction for *C. taxifolia*, *M. pyrifera*, and *F.v. mytili*. In the case of the well-
86 studied brown alga *Fucus vesiculosus* (Saha et al., 2014), effects of light and temperature have
87 been investigated independently through the study of the surface concentrations of three
88 metabolites [i.e. proline, dimethylsulfoniopropionate (DMSP) and fucoxanthin] known as
89 bacterial settlement inhibitors. The potential effect of the variations of these surface compounds
90 on the epibacterial community structure has been also studied. To our knowledge, this is the only
91 mesocosm study focusing simultaneously on surface microbiota and metabolites, with chemical
92 analyses specifically limited on these three compounds. The direct impact of both parameters
93 appears relatively limited on these metabolites, but variations of their surface concentrations
94 could possibly modify the relative proportions of major bacterial families, as shown when DMSP
95 concentration increases. However, if light and temperature seem to be key factors for shaping
96 the overall epibacterial community of marine algae, their combined effects have not been
97 investigated so far in controlled laboratory conditions, especially in relationships with the whole
98 surface chemical environment.

99 While most surface metabolites playing a potential role in the surface microbiome assembly (such
100 as DMSP or fucoxanthin) were presumably attributed to the host production (Lachnit et al., 2010;
101 Saha et al., 2011; Grosser et al., 2012; Saha et al., 2014), little is known on the relative importance
102 of bioactive compounds from the epibacterial community at the holobiont scale. These later,
103 could participate actively to the shift of a community structure, through antagonistic interactions
104 within the microbiome for example (antibiotic, quorum quenching activities, ...) (Wietz et al.,
105 2013). One of the most clear evidence of the role of microbial secondary metabolites on the host
106 was the morphogenesis-promoting factors required for the growth and morphogenesis in the
107 case of the sea lettuce *Ulva* spp. (Ghaderiardakani et al., 2017, 2019). *Taonia atomaria*
108 (Woodward) J. Agardh is an annual photophilic marine Phaeophyceae widely reported along the

109 Mediterranean and the NE Atlantic coasts (Guiry and Guiry, 2020). This seaweed is known to
110 produce at its surface several compounds displaying anti-adhesion activities (e.g. gleenol and
111 geranylgeranyl glycerol) (Othmani et al., 2016) against a panel of marine bacteria. Such
112 metabolites have been hypothesized to be part of the algal chemical defenses and involved in the
113 selection of a specific epibacterial community. Furthermore, strong seasonal correlations occur,
114 notably during spring and summer, between specific surface metabolites and some epibacterial
115 taxa (Paix et al., 2019). In the light of these results and those previously obtained for the algal
116 model *F.v. mytili*, the increase of temperature has been hypothesized as a key factor shaping the
117 dynamics of such interactions. However, in the case of *T. atomaria*, the field studies have not
118 delineated the respective effects of colinear factors such as temperature and light. Due to their
119 temporal covariations, their relative importance is now questioned according to the important
120 seasonal effect observed as part of *in situ* studies (Paix et al., 2019, *submitted*).

121 The objective of this “controlled conditions experiment” was to decipher the respective and
122 synergistic effects of temperature and irradiance on the interactions between *T. atomaria* and its
123 epibacterial community. The temperature values were chosen according to the natural *in situ*
124 variations observed during the summer, when the epibiotic community is stabilized (Paix et al.,
125 2019). As temperatures follow an increase and then a decrease from the beginning to the end of
126 the summer along coasts of north Brittany, three different temperatures were chosen: an
127 ambient one corresponding to the field measures in June (18°C named AT for ambient
128 temperature), together with a higher and a lower ones corresponding to the extremes observed
129 within this period (13°C and 22°C named LT and HT, respectively for low and high temperatures).
130 Additionally, the HT condition corresponded to +4°C compared to the AT condition, which suited
131 with the predictions made for 2081-20100 with the RCP 8.5 model in the Global Change context
132 (Collins et al., 2013). The different irradiance conditions were chosen in accordance with *in situ*
133 variations mainly linked to the different depths, according to the changing tide conditions, and
134 the range of photosynthetic saturation points (I_k) previously described in the literature for brown
135 seaweeds. Located at the limit between the intertidal and the infralittoral zones, *Taonia*
136 populations on Brittany coasts can vary from 2 to 8m depth. Consequently, contrasted degrees
137 of light penetration (according to the tide changes in this environment) were considered (Roberts

138 et al., 2018). Additionally, the three light treatments (20, 120 and 350 $\mu\text{mol photons m}^{-2} \text{s}^{-1}$,
139 named LI, AI and HI, respectively for low, ambient and high irradiances) were chosen since the
140 corresponding irradiance values were respectively located below, within and above the I_k range
141 generally observed for brown seaweeds (100 - 200 $\mu\text{mol photons m}^{-2} \text{s}^{-1}$) (Forster and Dring,
142 1994; Hanelt et al., 1995; Murakami et al., 2004). Such a choice was considered in order to
143 compare three different states of the seaweed based on its photosynthetic capacity.

144 These three temperatures and irradiances were combined and sampling was performed after
145 three different times of incubation after the acclimatation period (t_1 , t_2 and t_3 : one day, one week
146 and two weeks, respectively). The resulting surface microbiota and metabolome were subjected
147 to a multi-omics analysis. Untargeted LC-(+)-ESI-MS metabolomics dedicated to the analysis of
148 surface metabolites was coupled to 16S rRNA gene metabarcoding and flow cytometry, for the
149 analysis of epiphytic prokaryotic dynamics.

150

151 Results

152 Physicochemical parameters

153 Several physicochemical parameters measured in the aquaria showed a low variability during the
154 whole study, such as salinity, pH, dissolved O₂ levels, and [Si(OH)₄] with mean values of 35.8 ppt
155 [Standard deviation (SD) = ± 0.2 ppt], 8.1 (SD = ± 0.05), 90% (SD = ± 1.4%), and 1.93 μM
156 (SD = ± 0.28 μM), respectively (Table S1). However, some parameters showed a higher variability,
157 such as [NO₃⁻] and [PO₄³⁻] with mean values of 1.27 μM (SD = ±0.58 μM) and 0.209 μM
158 (SD = ±0.097 μM), respectively. Significant changes appeared only for [PO₄³⁻] according to the
159 three-way ANOVA test with the time factor only (Table S2), revealing an increase from t₁ to t₃
160 confirmed with a Tukey's test. No significant interaction between time, irradiance and
161 temperature factors was observed according to three-way ANOVA tests (Table S2). Moreover,
162 when comparing natural and aquaria seawater, only [Si(OH)₄] exhibited significant differences
163 (one-way ANOVA: *p* < 0.05), with mean values decreasing by a 3-fold factor from field to
164 controlled conditions (Table S1).

165 Physiological assessment

166 The maximum quantum yield of photosynthetic energy conversion (F_v/F_m) measured for all
167 samples showed mean values of 0.71 (SD = ± 0.1, Fig. S1A). Measures of thalli length showed
168 mean values of 16.6 cm (SD = ± 3.4, Fig. S1B). For these two parameters, three-way ANOVA tests
169 did not show any significant change whatever the conditions (sampling time, temperature, or
170 irradiance) whether considered independently or interacting (*p*-values > 0.05). As a proxy of the
171 light limitation stress for the seaweed, variations in the relative concentrations of mannitol (Fig.
172 S1C) revealed a significant interaction between time and irradiance factors (three-way ANOVA
173 tests, Table S2). However, no significant differences in the relative concentration of mannitol
174 were observed when comparing the sampling times, each other according to the multivariate
175 pairwise results (Fig. S1C). Moreover, no visible evidence of thalli deterioration (e.g., bleaching or
176 fragmentation) was observed throughout the time of the whole experiment.

177 Flow cytometry analyses

178 Abundances of heteroprocaryotic cells at the surface of *T. atomaria* were estimated through flow
179 cytometry and revealed densities ranging from 1.2×10^5 to 1.8×10^7 cells.cm⁻² (Fig. S2). When
180 comparing samples over time, a significant increase was observed from field to t₂ and then t₃
181 samples (Table S2, Fig. S2). However, no significant difference in cell densities were observed
182 between the different irradiance and temperature conditions (Table S2). No significant factors
183 interactions were also observed when considering the possible combinations between time,
184 temperature, and irradiance conditions (Table S2).

185 Epibacterial community diversity

186 NOCHL primers were recently designed for studies on algal-associated bacterial communities, to
187 avoid the contamination of 16S rRNA gene sequences from plastids (Thomas et al., 2020). In this
188 study, this combination was firstly compared to 515F-Y/926R primers, leading to similar patterns
189 of community structure (Fig. S3, details in SI, Mantel test at the order level: $p = 0.001$, $r = 0.8$).
190 NOCHL were chosen because no chloroplast 16S rRNA gene sequence was obtained, which could
191 have been a particular issue in this study due to the high number of sporophytes noticed at the
192 algae surface (details in SI).

193 While no difference appeared between field and t₀ samples, a global increase of the Shannon
194 index was observed over time from t₀ to t₃ (Fig. S4). More precisely, t₀ and t₁ samples exhibited a
195 significantly lower α -diversity in comparison with t₂ and t₃ samples. Moreover, at t₃ and for AI,
196 Shannon index showed significant lower values for samples at HT (Fig. S4, Table S2). Chao1 values
197 for field samples were significantly lower than those of all the controlled conditions samples (Fig.
198 S4, Table S2). At t₃, whatever the irradiance condition, Chao1 showed significant lower values for
199 HT samples compared to those at AT. At AI and HI, HT samples showed also lower values than
200 those of LT samples (Fig. S4, Table S2). No significant factor interactions were observed between
201 time, temperature and irradiance for both α -diversity indexes (Table S2).

202 Considering the β -diversity, the first axis of the weighted-Unifrac based NMDS revealed a global
203 shift from field to controlled conditions samples, despite a relatively high heterogeneity among
204 controlled conditions samples (Fig. 2A). Moreover, a shift of the prokaryotic community was

205 observed on the same axis over time from t_1 to t_3 samples (PERMANOVA test using the time
206 factor: $p = 0.001$, Table S3). The corresponding multivariate pairwise test showed that field, t_1 , t_2
207 and t_3 samples appeared significantly different from each other while t_0 samples were not
208 differentiated from field and t_1 ones (Table S4). On the second axis of the NMDS, differences
209 appeared according to temperatures with a cluster of HT samples distinct from AT and LT samples
210 (Fig. S5A, PERMANOVA test using the “Temperature” factor: $p = 0.001$, Table S3). A significant
211 interaction between time and temperature was also observed according to the PERMANOVA test
212 (Table S3). The three conditions (LT, AT and HT) appeared significantly distinct from each other
213 when compared with a multivariate pairwise test (Table S4). For irradiance, HI samples were
214 significantly differentiated from AI and LI ones, while no differences were observed between the
215 two latter groups. When considering t_1 , t_2 , or t_3 samples independently (Fig. 3), the resulting
216 NMDS plots showed separated clusters for each temperature (PERMANOVA and pairwise tests: p
217 = 0.001, Tables S3 and S4). However, no significant differences were observed within the three
218 irradiances for t_1 or t_2 samples (Table S4). Finally, t_3 samples were discriminated according to
219 irradiance as HI and LI samples were significantly different (Table S3 and S4).

220 A Venn diagram (Fig. S6) revealed that the percentage of OTUs and sequences shared between
221 all samples (field and controlled conditions samples) reached 53.8 and 88.7%, respectively. The
222 percentages of OTUs and sequences common to only controlled conditions samples (t_0 , t_1 , t_2 and
223 t_3) corresponded to 20 and 8.3%, respectively.

224 Considering the taxonomic affiliation of the epibacterial community, differences between field
225 and controlled conditions samples were observed at the family level, (Fig. S7). In field samples,
226 the main families observed were Hyphomonadaceae (Alphaproteobacteria), Alteromonadaceae,
227 Thiohalorbdaceae (Gammaproteobacteria) and Saprospiraceae (Bacteroidetes) representing 21,
228 15, 15 and 14 % of the community, respectively. Hyphomonadaceae appeared as a discriminant
229 taxon of field samples (LDA > 4, Table S5). Thioharlobdaceae and Hyphomonadaceae were mainly
230 represented by the genera *Granulosicoccus* and *Litorimonas* contributing up to 8 and 6% to the
231 dissimilarity between field and t_0 samples, respectively (Table S6).

232 In contrast, the community structure of controlled conditions samples was mainly characterized
233 by the occurrence of Alteromonadaceae and Rhodobacteraceae with relative percentages
234 ranging from 9 to 61% and 9 to 44%, respectively (Fig. S7). The Alteromonadaceae family
235 appeared mainly represented by the genera *Alteromonas* and *Paraglaciecola* which were
236 discriminant taxa specific to t_0 samples (Table S5) and contributed to 13 and 3% of the overall
237 dissimilarity between field and t_0 samples, respectively (Tables S6).

238 From t_0 to t_3 , and whatever the temperature/irradiance conditions, a clear decrease of
239 Alteromonadaceae and an increase of Spongiibacteraceae, Rhizobiaceae (mainly represented by
240 the genus *Lentilitoribacter*) and Cellvibrionaceae was noticed (Fig. S7). These three latter families
241 appeared as discriminant taxa specific to t_3 samples (LDA > 4, Table S5).

242 For the analysis of discriminant taxa, a focus was made on t_3 samples since it was expected to
243 offer the most marked differences in line with the changing conditions (Table S7 ; Fig. 4 ; Fig. S8).
244 Actually, the highest number of discriminant taxa of a specific irradiance/temperature condition
245 for a same LDA threshold was observed for t_3 , whatever the taxonomical rank. More precisely,
246 for thresholds of 3.4 and above, t_3 samples gathered approximately two and four times more
247 discriminant genera than t_2 and t_1 samples, respectively. Overall, discriminant taxa specific of t_3
248 samples mostly differed according to the temperature (Fig. 4). The genus *Oleiphilus* occurred
249 mainly among LT samples, whatever the irradiance, and appeared as an example of taxa
250 displaying a similar trend for t_1 and t_2 samples (Fig. S8). Several other genera showed a similar
251 tendency under particular conditions of irradiance, such as *Kordia* at AI and *Neptuniibacter* at LI.
252 In contrast, some genera occurred mainly in samples at HT, such as *Sulfitobacter*, *Congregibacter*
253 and *Parvularcula* at AI, *Hirschia* at LI, *Congregibacter* and *Parvularcula* at HI. Moreover, some
254 genera also differed according to the irradiance conditions, such as *Kordia* at LT which occurred
255 mainly at AI compared to LI and HI. At HT, *Lentilitoribacter* and *Parvularcula* were found in
256 significantly higher percentages at HI compared to LI. A similar tendency was observed for
257 samples subjected to AT for the genus *Jannaschia*.

258 Surface metabolome fingerprinting and variations of discriminant metabolites

259 When all samples were included, differences of surface metabolome profiles between field and
260 controlled conditions samples appeared on the second component of the PCA score plot (Fig. 2B).
261 Moreover, a global shift of the surface metabolomes was observed over time on the first
262 component from t_1 to t_3 . Finally, a discrimination was also observed on the second component of
263 the PCA between HI and LI samples (Fig. S5B). The PERMANOVA test conducted with the three
264 experimental factors (time, temperature, and irradiance) validated significant differences within
265 each factor, but also a significant interactive effect of the three factors (Table S8). The multivariate
266 pairwise analysis revealed at first that all sampling times were significantly different from each
267 other except t_3 with field, t_0 and t_2 on one hand, and t_1 with t_0 on the other hand (Table S9). When
268 comparing the three groups of samples obtained with different irradiances, all of them were
269 significantly different from each other, while for temperature conditions, HT samples were
270 significantly discriminated from AT and LT samples on the basis of their surface metabolome.

271 The PCA plot obtained only with the t_1 samples did not reveal any clear differences between the
272 temperature/irradiance conditions (Fig. 5). However, multivariate tests showed that LI and HI
273 samples were statistically different (Table S9). In the case of t_2 samples, the resulting PCA plot
274 (Fig. 5) allowed to discriminate: (i) HT samples from the two other temperature conditions on the
275 first component, (ii) on the second component, LI from HI samples (PERMANOVA tests with
276 “temperature” or “irradiance” factors: $p = 0.001$, Table S8). Pairwise comparisons showed
277 significant differences between HT samples and those at the two other temperatures on one
278 hand, and between LI samples and those obtained at the two other irradiances on the other hand
279 (Table S9). Finally, the corresponding PCA plot (Fig. 5) for t_3 samples showed a discrimination
280 between HI and LI samples on one hand, and between HT and LT samples on the other hand. In
281 term of pairwise comparisons, samples were significantly different between each temperature
282 (Tables S9). LI samples appeared also significantly different from samples obtained at the two
283 other irradiances (Table S9). Moreover, the interaction of temperature and irradiance was found
284 to be significant only for t_3 , in contrast to the two previous sampling times (Table S8).

285 When comparing field and t_0 samples, the most discriminant compounds identified according to
286 their Variable Importance in Projection (VIP) scores were fucoxanthin (VIP score: 1.87) and

287 phenylalanine (VIP score: 1.85). These two compounds were more produced in t_0 samples
288 compared to field samples (Fig. S9) with a fold change of 7.0 and 6.2, respectively.

289 Subsequently, a focus was made on the variations of a panel of annotated and discriminant
290 surface compounds (Fig. 6; Fig. S9; Table S10) differentially expressed in t_3 samples according to
291 each condition (VIP score > 0.6), since this sampling time offered the largest number of significant
292 and discriminant variations. Such variations were not systematically observed in samples
293 collected at previous sampling times (Fig. S9).

294 At LT, DMSP, mannitol, several diacylglycerylhydroxymethyl-*N,N,N*-trimethyl- β -alanine (DGTAs)
295 [such as DGTA (C42:11), DGTA (C40:8), DGTA (C36:4) and DGTA (C36:9)] and a diacylglycerol [DG
296 (C36:9)] were found in higher concentrations in HI samples compared to those at LI. Moreover,
297 mannitol and DGTA (C36:4) were also more produced in AI compared to LI, while DGTA (C42:11)
298 and DG (C36:9) were found in higher concentrations at HI rather than AI. At AT, mannitol was
299 found in higher amounts at AI and HI rather than at LI and gleenol was also found in higher
300 concentrations in AI rather than at LI. A quite opposite tendency was observed for fucoxanthin
301 which appeared in higher amounts in samples at LI compared to those obtained at HI. At HT,
302 fucoxanthin, tryptophan and an unknown sesquiterpene with the molecular formula $C_{15}H_{18}O_2$
303 were produced in lower concentrations in samples at LI rather than those at HI while the opposite
304 tendency was observed for mannitol.

305 At LI, DGTA (C36:4), gleenol and phenylalanine were more produced in HT samples rather than
306 those at LT. At AI, proline betaine and DG (C36:9) were found in higher concentrations in LT
307 samples compared to HT ones. DG (C36:9) was also more produced in samples at LT compared to
308 those obtained at AT. Gleenol was found in higher concentrations at AT than at HT. At HI, DGTA
309 (C42:11) and DGTA (C36:0) were produced in higher concentrations in LT samples compared to
310 AT and HT samples.

311 Discussion

312 In a general context of global change, the impact of environmental factors on the surface
313 microbiota of marine holobionts is still poorly studied through controlled conditions experiments
314 and the combination with the surface host's metabolome characterization remains rare. In the

315 case of *T. atomaria*, the concurrent temporal increase of temperature and irradiance has been
316 hypothesized to play a key role in controlling seaweed-microbiota interactions in natural
317 environment (Paix et al., 2019, Paix et al., *in prep.*), while a decrease of these parameters had
318 been never investigated before. The aim of this study was to decouple these two factors to
319 understand their specific and synergistic effects on the host-surface microbiota interactions.

320 Through this study, we also aimed to confirm the efficiency of NOCHL primers to avoid plastid 16S
321 rRNA gene amplification. Their amplification led to a decrease of the sequencing depth for
322 prokaryotic 16S rRNA sequences which can prevent a full assessment of the diversity of
323 prokaryotic communities associated to plants or algae. We compared this set of primers with
324 515F-Y/926R primers which previously lead up to 36% of chloroplast 16S rRNA gene sequences
325 (Paix et al., 2020). We confirmed the results from Thomas et al., 2020, since the efficiency of
326 NOCHL primers was clearly observed with no sequences affiliated to chloroplasts.

327 [Conditioning effect on the holobiont system](#)

328 Heteroprokaryotic densities and richness of the epiphytic community appeared higher for
329 controlled conditions samples after the one-week acclimation period compared to field ones. A
330 difference in β -diversity was also observed between these two sets of samples. Besides, a
331 relatively high percentage of OTUs number (20%) were specific to controlled conditions samples.
332 However, these specific OTUs represented a lower proportion in terms of sequences (8.3%),
333 compared to their percentage based on the number of OTUs. Two plausible scenarios could
334 explain the presence of such epibionts at the surface of controlled conditions samples despite
335 they had not been observed within field samples. Firstly, these OTUs could be rare taxa in field
336 samples, removed with the 0.005% filtering process of the FROGS pipeline (used for filtering the
337 sequencing artefacts, Bokulich et al., 2013) or with the rarefaction of the OTU-table. These taxa
338 may benefit from the algal conditioning and become more abundant at the algal surface in
339 aquaria. Another source could be the pre-filtration process of the running seawater. Once
340 pretreated, the running coastal seawater provided to the aquarium device was filtered (with
341 ultimately 1 to 3 μm filters) and then sterilized using UV radiations. However, despite these
342 filtration steps, some exogenous colonizers might come from the planktonic community from the
343 coastal sea, or also from biofilms on the surfaces of the experimental devices (e.g. tubes or filters).

344 Considering these two scenarios, it cannot be excluded that these rare or/and exogenous taxa
345 may also benefit from the change of uncontrolled and/or not measured parameters throughout
346 the experiment. Such hypothesis might explain the significant interaction observed between time
347 and temperature factors and could be considered as a limitation for this study, raising the
348 importance of monitoring a large panel of environmental parameters to adjust and improve the
349 stability of the experimental setup.

350 The effect of a controlled conditioning on the surface microbiota was already investigated for the
351 Rhodophyta *Delisea pulchra* and a similar scenario was also proposed by the authors (Zozaya-
352 Valdés et al., 2016). 15 days after the transfer of *D. pulchra* from field to aquaria, a change of
353 microbiota structure was observed with specific enriched OTUs. The main ones were affiliated to
354 Kordiimonadales (mainly the genus *Kordiimonas*), Alteromonadales (mainly the genus *Glaciecocola*)
355 and Cytophagales. In our study, the main taxa promoted after one week of acclimation also
356 belonged to Alteromonadales with the genera *Alteromonas* and *Paraglaciecocola*. Several strains
357 belonging to these two genera have been previously described for their ability to degrade
358 seaweed polysaccharides (Akagawa-Matsushita et al., 1992; Schultz-Johansen et al., 2016; Bech
359 et al., 2017). Moreover, the genus *Alteromonas* was already identified as increasing during
360 mesocosm experiments (Schäfer et al., 2000). *Alteromonas macleodii* in particular is well known
361 as a r-strategist, possibly taking advantage of nutrient-enriched environments (Zemb et al., 2010;
362 Romera-Castillo et al., 2011; Tada et al., 2011; Lawes et al., 2016). Despite we used a
363 metabolomics approach which did not allowed to investigate algal polysaccharides, we
364 hypothesized that a shift of the global chemical composition at the algal surface (e.g. an increase
365 of polysaccharides biosynthesis) after the conditioning might constitute a selective advantage for
366 *Alteromonas* and *Paraglaciecocola* spp., which could metabolize such a carbon source and quickly
367 grow at the surface of *T. atomaria*.

368 In contrast, two other genera of the Alteromonadales, *Litorimonas* and *Granulosicoccus* spp.
369 significantly decreased when algal samples were transferred in aquaria. These two genera have
370 been already described at the surface of *T. atomaria* as specific, core and pioneer taxa and are
371 known to quickly decrease over time on Mediterranean sites (Paix et al., 2019, 2020, Paix et al.,
372 *submitted*). Even if environmental conditions from the sampling site of this study clearly differ

373 from those of the Mediterranean ones, these taxa could be sensitive to environmental changes.
374 Among changes mediated by the conditioning from field to mesocosms, decrease of
375 hydrodynamics and modification of the selective pressure associated to predation or viral lysis
376 might constitute crucial factors (Cram et al., 2016).

377 For the surface metabolome, several metabolites were differentially produced after the transfer
378 of *T. atomaria* from field to aquaria. For example, phenylalanine and fucoxanthin were observed
379 with higher concentrations after the transfer in aquaria while field samples were characterized
380 by a higher expression of DGTAs. Within diverse algal species, phenylalanine and fucoxanthin
381 production is known to increase with higher UV-B radiations (Heo and Jeon, 2009; Hartmann et
382 al., 2015). Hence, the metabolomics shift linked to the transfer of *T. atomaria* from field to
383 aquaria, might be explained by a change of light conditions/quality associated to the LED/filter
384 system. As hypothesized for polysaccharides, such chemical variations at the algal surface might
385 also be considered as potential factors shaping differences of epibacterial composition.

386 Finally, the physiological assessment of the macroalgae was more generally determine through
387 analyses of the algal growth, the relative concentration of mannitol, and the maximum quantum
388 yield of PSII (F_v/F_m). Linked to the algal photosynthetic activity, these two latter parameters aimed
389 to decipher the light limitation of CO₂ fixation, and the photosynthetic efficiency of the seaweed.
390 The variations of the mannitol concentrations during the experiment suggested that
391 photosynthetic CO₂ fixation appeared mainly linked to irradiance level during the experiment and
392 was limited according to the sampling times when compared independently. Moreover, F_v/F_m
393 values did not changed significantly whatever the factors considered. Similarly, the algal growth
394 assessed through the measurement of thalli samples, did not showed any significant differences
395 neither with time, irradiance, or temperature conditions. Hence, regardless of conditions of
396 irradiance and temperature, these results suggested a relative stable physiological status of the
397 seaweed throughout the experiment.

398 **Short-term responses of algal surface microbiota and metabolome**

399 Through multivariate analyses conducted within t_1 samples, the short-term responses (24h) of
400 the surface microbiota and metabolome were found to clearly differ. On one hand, short-term

401 differences of prokaryotic β -diversity only appeared with the change of temperature (increase
402 and decrease). More particularly, the *Oleiphilus* genus was a major discriminant taxon which
403 differed after t_1 , with higher percentages at LT compared to AT and HT. Conversely, the absence
404 of a direct effect of irradiance on the global structure of the bacterial community at t_1 could be
405 linked to the absence of major phototrophic taxa in the initial community. The NOCHL primers
406 did not allow to amplify sequences of 16S rRNA gene from Cyanobacteria (Thomas et al., 2020).
407 However, Cyanobacteria sequences constituted less than 0.1% of the overall community for
408 samples tested (t_0 and t_1) with the 515F-Y/926R primers. Moreover, when focusing on aerobic
409 anoxygenic phototrophs [AAP, a functional group gathering various subgroups within Alpha-,
410 Beta- and Gammaproteobacteria, composed of facultative photoheterotrophs which use
411 bacteriochlorophyll to harvest light energy (Koblížek, 2015)], the main genera identified in the
412 dataset were *Roseobacter*, *Congregibacter*, *Erythrobacter* and *Jannaschia*, but these genera
413 represented less than 0.01% of all the sequences and did not vary significantly according to
414 irradiance conditions in t_1 samples. Moreover, the absence of a direct effect of irradiance changes
415 at t_1 on the epibacterial community could be explained by the fact that the growth of these main
416 phototrophic taxa would require a longer period (e.g. one week or more, see the next section
417 below on long-term effects).

418 On the other hand, short term differences between surface metabolomes were observed only
419 when the irradiance conditions varied. The highest irradiance rapidly induced an increase of the
420 production of mannitol at the algal surface. This polyol is a photosynthetic product which
421 constitutes the main form of energy storage for brown algae (Lehvo et al., 2001; Rousvoal et al.,
422 2011; Weinberger et al., 2011) and a similar observation has previously been made for *F.*
423 *vesiculosus* (Saha et al., 2014).

424 Interestingly, these results indicated that the short-term responses of the two components of the
425 holobiont system are not susceptible to the same factor. Consequently, we hypothesized this
426 change of algal host and surface microbiota would correspond to responses firstly inherent to
427 their respective physiological specificities, and that reciprocal interactions at the holobiont scale
428 could only occur later. An interesting approach to confirm that irradiance could constitute a
429 primary and direct parameter acting on the algal host, in contrast to the temperature, would be

430 to work on similar experiments with an axenic host as suggested by van der Loos et al., 2019.
431 Despite the methodological complexity of cultivating such a model, this type of study would allow
432 to decouple factors effects on the host without the risk that epibiotic bacterial metabolites
433 interfere.

434 [Effect of irradiance on surface microbiota: an indirect long-term effect mediated by the algal host?](#)

435 After the conditioning, differences appeared only after two weeks between samples exposed to
436 HI and LI, and this even more in the case of HT. The genera *Lentilitoribacter*, *Parvularcula*,
437 *Congregibacter* (at HT), and *Jannaschia* (at AT) constituted taxa which seemed to be especially
438 adapted to higher irradiance. *Pelagimonas* and *Kordia* were genera especially adapted to AI
439 conditions in the case of HT and LT, respectively. The case of *Jannaschia* and *Congregibacter* is
440 interesting since one species is known to produce the bacteriochlorophyll *a* pigment and is
441 described as an AAP (Fuchs et al., 2007; Yoon et al., 2010; Pujalte et al., 2014; Selyanin et al.,
442 2016). Higher irradiances could have constituted a beneficial condition thanks to its phototrophic
443 metabolism, and the delayed response is consistent with clear effects of light observed on natural
444 AAP communities in the long terms (Koblížek, 2015). As no evidence of phototrophic metabolism
445 was observed for *Parvularcula*, *Pelagimonas* and *Kordia*, irradiance could then constitute an
446 indirect factor explaining the selection of these taxa. Moreover, it was clearly established that
447 surface metabolome was directly impacted by the irradiance changes during the whole
448 experiment. Consequently, several surface algal metabolites differentially expressed according to
449 light intensity could be considered as potential factors shaping microbiota light-dependent
450 differences with time.

451 After two weeks, mannitol, fucoxanthin and DMSP were the main metabolites involved in the
452 surface metabolome changes in connection with irradiance conditions. As already observed after
453 one day, mannitol remained discriminant but with increasing concentrations in the case of HI,
454 which may still result from a higher algal photosynthetic activity. Mannitol constitutes a
455 preferential source of carbon for a large bacterial diversity but it is also a compatible solute known
456 to play a role in osmoprotection (Kets et al., 1996; Sand et al., 2013; Zahid et al., 2015). Mannitol
457 catabolism has been notably investigated through a genomic approach with *Zobellia*
458 *galactanivorans*, a Flavobacteriia closely associated to several macroalgae (Barbeyron et al.,

459 2001; Groisillier et al., 2015). The operon associated to mannitol assimilation for this bacterial
460 strain has been identified and also found in other genomes among Flavobacteriaceae (Groisillier
461 et al., 2015). Interestingly, this bacteria has the ability to degrade various algal polysaccharides
462 such as alginates and fucans of Ochrophyta, or agars and carrageenans of Rhodophyta (Thomas
463 et al., 2012, 2013; Barbeyron et al., 2016). In addition to mannitol, algal polysaccharides could
464 also constitute an important source of carbon for epiphytic bacteria particularly adapted to
465 macroalgal niches (Gobet et al., 2018). Consequently, such primary or secondary products of the
466 algal photosynthesis could then be considered as key factors involved in epibacterial communities
467 shaping, especially in the case of changing irradiance. An interesting perspective would be to
468 investigate the polysaccharide production of *T. atomaria*, notably under distinct irradiances and
469 to focus on microbial functions associated with the degradation of such biopolymers.

470 For fucoxanthin, a higher expression was observed in the case of a LI. Increasing amounts of this
471 carotenoid have been observed with depth or shade increase in other macroalgae such as *F.*
472 *vesiculosus*, *Ascophyllum nodosum*, *Udotea petiolate*, and *Dictyota dichotoma*. These data
473 illustrating the adaptation of the photosynthetic performances of seaweeds with a lower quantity
474 and quality of light (Ramus et al., 1977; Perez-Bermudez et al., 1981). Here, we suggested that a
475 similar shade-light adaptation occurred in *T. atomaria* to compensate the irradiance decrease.
476 Through culture dependent approaches, fucoxanthin was also found to display inhibiting activities
477 against bacterial adhesion (Viano et al., 2009; Saha et al., 2011). However, the selective effect of
478 fucoxanthin on the epibacterial community structure of macroalgae is always a matter of
479 discussion (Lachnit et al., 2010; Saha et al., 2011; Egan et al., 2013). In Saha et al., 2014,
480 correlations between fucoxanthin and several bacterial taxa were investigated and several
481 “fucoxanthin-positive” and “-negative” taxa have been determined. The Flavobacteriaceae family
482 was notably found positively correlated to fucoxanthin suggesting that members of this family
483 could be attracted by this compound. Here, no clear correlation was observed between
484 Flavobacteriaceae and fucoxanthin (linear regression: $R^2 < 0.2$). Through *in vitro* and *in vivo* field
485 experimental approaches, the anti-adhesion activity of fucoxanthin and of potentially
486 unidentified compounds of a non-polar fraction of the surface extracts of *F. vesiculosus*, has been
487 previously supported. However, fucoxanthin has not been found to impact the community

488 structure of *F. vesiculosus* and cautions have been raised to avoid any premature causality links
489 (Lachnit et al., 2013). A low selective range of activity may be important to consider (Egan et al.,
490 2013) and further investigations still need to be conducted to clearly understand the effect of
491 fucoxanthin on macroalgal epibacterial communities under ecological relevant conditions.

492 In a previous work on Mediterranean samples of *T. atomaria*, DMSP was found to increase at the
493 algal surface from February to July and such a variation was hypothesized to be correlated with
494 the temporal increase of temperature and/or irradiance (Paix et al., 2019). In the present study,
495 DMSP increased significantly with the irradiance intensity in the case of LT conditions. The DMSP
496 concentrations of total extracts have been previously investigated under different light conditions
497 in other seaweeds, such as the green algae *Ulothrix implexa*, *Ulothrix subflaccida*, *Enteromorpha*
498 *bulbosa*, *Acrosiphonia arcta*, *Ulva rigida*, *Blidingia minima* (Karsten et al., 1990, 1992), *Ulva*
499 *lactuca* (Van Alstyne and Puglisi, 2007), *Codium fragile* (Lyons et al., 2010) and the brown alga *F.*
500 *vesiculosus* (Saha et al., 2014). In accordance with our results, Karsten et al., 1990, 1992 and Lyons
501 et al., 2010, have found in their respective algal models that DMSP concentrations were higher
502 with an increasing irradiance. Taken together, these results may strengthen the hypothesis of a
503 light-dependent DMSP biosynthesis, especially in the case of low temperature conditions (Karsten
504 et al., 1992). Moreover, DMSP is also produced by many microalgae, including dinoflagellates and
505 diatoms (Bullock et al., 2017), and the potential origin of DMSP at the surface of *T. atomaria* could
506 also be linked to such epiphytes that were identified on several Dictyotaceae including *T.*
507 *atomaria* (Ternon et al., 2020). Besides, DMSP constitutes a source of carbon and sulfur for a large
508 diversity of bacteria, especially those from the *Roseobacter* clade (Howard et al., 2008; Curson et
509 al., 2011; Dogs et al., 2017). DMSP is also known as a chemo-attracting compound released at the
510 surface of *Ulva mutabilis* which allows the “gardening” and mutualistic interactions with
511 *Roseovarius* sp. (Wichard et al., 2015; Kessler et al., 2018). At the surface of *T. atomaria*, several
512 discriminant taxa such as *Sulfitobacter* and *Jannaschia*, specific to a condition of temperature and
513 irradiance at t₃, have been already described for their DMSP catabolic activity (Mou et al., 2005;
514 Curson et al., 2008; Howard et al., 2008). More precisely, an interactive effect of temperature and
515 irradiance was observed for the genus *Jannaschia*, with a maximum abundance under HI and AT
516 conditions as mentioned above. Then, the higher DMSP production induced by a higher irradiance

517 could also positively affect the growth and development of members of this genus at the surface
518 of *T. atomaria*.

519 Effect of temperature on the holobiont dynamics

520 The increase of seawater temperature was predicted to potentially affect macroalgae health at a
521 global scale (Egan and Gardiner, 2016; Bindoff et al., 2019; van der Loos et al., 2019). At the
522 holobiont scale, temperature affects microbial shifts for a large number of seaweeds in controlled
523 condition studies, such as *D. pulchra* from the Tasman sea (Zozaya-Valdés et al., 2016),
524 *Neogoniolithon fosliei* from the Coral sea (Webster et al., 2011), *Macrocystis pyrifera* from NE
525 Pacific coasts (Minich et al., 2018), *Amphiroa gracilis* from the SE Indian ocean (Huggett et al.,
526 2018), *Fucus vesiculosus f. mytili* from the North sea (Mensch et al., 2016) and *F. vesiculosus* from
527 the Baltic sea (Stratil et al., 2013). Concerns are notably raised since lower health conditions and
528 chemical defenses caused by increasing temperature can result to a microbiota dysbiosis (Egan
529 et al., 2014; Egan and Gardiner, 2016; Minich et al., 2018). More precisely, the development of
530 opportunistic pathogens could be promoted through the activation of virulence factors (Case et
531 al., 2011; Fernandes et al., 2011; Gardiner et al., 2017).

532 Among epiphytic bacteria which are known to be favored by an increase of seawater
533 temperature, the Rhodobacteraceae family is particularly represented (Case et al., 2011;
534 Fernandes et al., 2011; Stratil et al., 2013; Saha et al., 2014; Qiu et al., 2019). In the case of *D.*
535 *pulchra*, pathogens from the Roseobacter group have been particularly observed, especially for
536 bleached algae under high temperature conditions (Case et al., 2011; Zozaya-Valdés et al., 2015,
537 2016). However, pathogens of *D. pulchra* are not specifically restricted to this family (Kumar et
538 al., 2016). In the present study, Rhodobacteraceae family appeared to be the main family
539 increasing with the temperature, with notably the genus *Sulfitobacter*. Interestingly, the genus
540 *Sulfitobacter* was also found to be positively correlated to the temperature at the surface of *M.*
541 *pyrifera* harvested [BP1][c2] on the Chilean coasts (Florez et al., 2019). Attention was also paid on
542 variations of several taxa from this family known as potential pathogens, such as *Nautella*,
543 *Phaeobacter* and *Aquimarina* (Fernandes et al., 2011; Kumar et al., 2016). The contribution of
544 these potential pathogens to the overall microbiota shift in response to an increase of

545 temperature was not significant. Moreover, no clear disease event (bleaching, blistered or
546 disrupted tissues) was observed on thalli of *T. atomaria* during the whole study.

547 However, a lower α -diversity in terms of richness, was observed when temperature increases.
548 Considering that a decrease of richness but not diversity (in HI and LI conditions) might indicate a
549 loss of “rare” taxa, this change of α -diversity could constitute a transient phase before a newly
550 more diversified and stable state.

551 However, in the case of human holobiont, a decrease of α -diversity constitutes a sign of a
552 potential dysbiosis (Pitlik and Koren, 2017). For marine holobionts, including seaweeds, a high
553 diversity is often considered to be essential for the stability and the resilience of the holobiont
554 system under changing conditions (Loreau et al., 2001; Moore, 2005; Longford et al., 2019).
555 Consequently, even if no clear pathogens were identified at the surface of *T. atomaria*, a
556 decreasing richness under higher temperatures may suggest a lower fitness of the holobiont.

557 A global shift of the β -diversity of the surface microbiota of *T. atomaria* was observed after one
558 day under high temperature conditions while modifications of the surface metabolome were only
559 observed after one week. For the β -diversity, significant interactions were observed between
560 time and temperature, suggesting a continuous shift toward a stable structure occurring after a
561 long-term period. For the metabolome, significant interactions between temperature and
562 irradiance were observed only at t_3 . We hypothesized that temperature may directly modify the
563 microbiota community structure over time and later induce an adaptive response of the algal
564 metabolome which in turn regulate the epibiosis. In Othmani et al., 2016, the anti-adhesion
565 activity of several sesquiterpenes found at the surface of *T. atomaria* has been investigated
566 against several bacterial strains isolated from marine biofilms. The gleenol, a spirooxane
567 sesquiterpene, has shown strong anti-adhesion activities at relevant natural concentrations. This
568 compound has been proposed to play an important role on the chemical selection of a specific
569 microbial community at the surface of *T. atomaria* (Othmani et al., 2016). In the present study,
570 the amounts of gleenol at the algal surface appeared to reach their maximal level at HT/LI and
571 AT/AI for t_3 samples. The differential production of this metabolite could possibly constitute a

572 host adaptation to limit quantitatively and/or qualitatively the dynamics of the microbiota
573 composition induced by the change of temperature.

574 Changes of the surface metabolome of *T. atomaria* linked to temperature variations could also
575 be attributed directly to physiological processes inherent to the algal host. Among other
576 metabolites which differ significantly according to temperature, several polyunsaturated
577 membrane lipids were identified, including diacylglycerols (DGs) and DGTAs. These lipids were
578 mainly expressed in the case of LT. Here, we hypothesized that thalli of *T. atomaria* exposed to
579 HT express less polyunsaturated lipids in order to decrease the fluidity of its membrane. Such
580 changes in membrane lipid composition for seaweeds has been already described as a mean to
581 maintain an optimal membrane fluidity under changing temperature conditions (Eggert, 2012).
582 Besides, this process is also well known in the case of microalgae (Sato and Murata, 1980, 1982;
583 Schüler et al., 2017). This adaptation to temperature change could thus play a crucial role to
584 maintain the integrity of several membrane process, including enzymatic mechanisms such as the
585 induction of heat-shock genes during the membrane rigidification of *Synechocystis* (Inaba et al.,
586 2003; Los and Murata, 2004; Eggert, 2012).

587 Conclusion

588 To our knowledge, this is the first multi-omics study, coupling untargeted metabolomics and 16S
589 rRNA gene metabarcoding, to study a seaweed holobiont responses to experimentally controlled
590 environmental conditions. Through such an approach, we showed that the seaweed-holobiont
591 dynamics of the Phaeophyceae *T. atomaria* was shaped by both temperature and irradiance. The
592 response to temperature changes appeared to be faster for the microbiota than for the
593 metabolome at the surface of the alga. Conversely, irradiance changes may impact firstly the algal
594 surface metabolome and, only then, its associated microbiota. We suggested that indirect effects
595 could occur only after few days. Algal metabolome variations resulting from a differential
596 photosynthetic activity induced by a shift of irradiance could be a factor shaping thereafter the
597 epiphytic microbiota. Several metabolites, such as mannitol, fucoxanthin and DMSP, known to
598 play important roles on seaweed-microbiota interactions could be involved. Overall, bacterial
599 richness appeared lower in the case of a higher temperature with a positive selection of several
600 specific taxa (notably from the Rhodobacteraceae family), probably taking advantage over other

601 families (such as Oleiphilaceae and Flavobacteriaceae, mainly represented by the genera
602 *Oleiphilus* and *Kordia*, respectively). These results suggested to better investigate the algal fitness
603 in future studies.

604 Experimental procedures

605 Aquarium experimental device

606 The whole experimental device was set up at the “Roscoff Aquarium Services” structure (Centre
607 de Ressources Biologiques Marines, Station Biologique de Roscoff, France) in a thermostated
608 room at 16°C. The room had three shelves, each of them with three floors. Each floor gathered
609 three replicate aquaria (15L each), resulting in a total of 27 aquaria (Fig. S10 and S11). Each shelves
610 system was supplied by the same independent semi-open water circuit with pre-treated running
611 seawater pumped from Roscoff coasts [details of pre-treatment in Supplementary information
612 (SI)]. At first, the pre-treated seawater went through an independent 50L tank for each shelf and
613 was UV-treated with a Reeflex UV 800 system (Eheim, Deiziau, Germany). The water temperature
614 within each tank was conditioned by TK500/TR10 chiller/heater systems (TECO refrigeration
615 technologies, Ravenna, Italy). Seawater was then distributed to each aquarium through a
616 Compacton 2100 pump (Eheim). When arriving to aquaria, the mean water flow was 36.5 L h⁻¹
617 (SD = ±7.5). Finally, the water from each aquarium went back by overflowing to the first tank
618 through a micron bag (100 μm; Red Sea, Düsseldorf, Germany). Two rows of 12V LED ribbons (LED
619 5050, Inovatlantic, Nantes, France) were set up on the top of each floor resulting in an irradiance
620 of 120 μmol photons m⁻² s⁻¹ measured at the bottom of each aquarium (SD = ±8.1). This
621 irradiance intensity corresponds approximatively to the mean *in situ* irradiance going up to 5m
622 depth on NW French Atlantic coasts in summer (Martin et al., 2006). Each light system was set on
623 a 16h:8h light:dark cycle during the whole experiment, which corresponds to the natural
624 day:night cycle at that time. To avoid any position bias between aquaria, particular cautions were
625 taken when LED ribbons were set up, to ensure a homogenous irradiance intensity for each
626 replicate of aquarium within the floors, during the whole experiment (SD < 9%). Additionally,
627 external source of irradiance or heat from the thermostated room were avoided by keeping the
628 room in the dark and each floor closed by a specific door.

629 Sampling and biological material

630 Approximatively 120 thalli of *Taonia atomaria* (Woodward) J. Agardh (Dictyotaceae,
631 Phaeophyceae) were collected by diving at Guimaëc (The Channel, 48°41'39.9"N 3°41'50.7"W) in

632 July 2018 at low tide (2 to 4m depth). Thalli were stored in cool boxes filled with surrounding
633 seawater and transported at lab within one hour after sampling.

634 Once at lab, only thalli with a length between 20 and 30 cm were kept considering only individuals
635 within the same development period. Furthermore, thalli showing evidence of macrofouling at
636 their surface were not considered and ultimately a total of 87 thalli were kept. Among them, three
637 thalli haphazardly selected were considered as triplicates of field samples and directly used for
638 cytometry, metabarcoding and metabolomics analyses.

639 **Controlled conditions experiment**

640 The 84 remaining thalli were haphazardly selected and distributed in the 27 aquaria as described
641 in Fig. 1. The whole study was conducted with triplicates of aquaria for each condition. For each
642 thallus, holdfasts were carefully attached to stainless steel screws in order to ballast the thallus
643 at the bottom of the aquarium. The seawater temperature and the irradiance intensity in all
644 aquaria were set to field conditions at 18°C (SD = ± 0.2) and 120 $\mu\text{mol photons m}^{-2} \text{ s}^{-1}$
645 (SD = ± 10.5), respectively, and used for an acclimation period of one week. At the end of the
646 acclimation (t_0), three replicates were sampled (t_0 samples, Fig. 1) and analyzed. After this
647 sampling, all the aquaria contained three thalli (on for each following sampling times) and the
648 conditioning period was started with 9 distinct conditions: three temperature coupled with three
649 irradiances. The three chiller/heater systems from each shelf were set to 13°C (SD = ± 0.6), kept
650 to 18°C (SD = ± 0.2) or set to 22°C (SD = ± 0.5). These “low”, “ambient” and “high” temperature
651 conditions were named LT, AT and HT, respectively. The change of temperature was progressively
652 done during 3h. For each floor, the irradiance of (i) bottom floors was set to 20 $\mu\text{mol photons m}^{-2}$
653 s^{-1} (SD = ± 0.75) by adding a solar film (F339-2000 , d-c Fix®), (ii) mid floors was kept to 120 μmol
654 $\text{photons m}^{-2} \text{ s}^{-1}$ (SD = ± 10.5), (iii) top floors was set to 350 $\mu\text{mol photons m}^{-2} \text{ s}^{-1}$ (SD = ± 10.6) by
655 turning on two supplementary LED ribbons. These “low”, “ambient” and “high” irradiances
656 conditions were named LI, AI and HI, respectively.

657 One day after, one thallus per aquarium was chosen haphazardly and sampled, consisting in 27 t_1
658 samples (9 cross-conditions in triplicates, Fig. 1). One and two weeks after t_0 , two other samplings
659 were performed in the same way with 27 t_2 and 27 t_3 samples, respectively (Fig. 1). For all

660 sampling points, each replicate of sample (i.e. an individual thallus) was subjected to four types
661 of analyses : (i) measurement of maximum quantum yield [F_v/F_m] of photosynthetic energy
662 conversion, (ii) flow cytometry, (iii) 16S rRNA gene metabarcoding, (iv) and UHPLC metabolomics
663 analyses, using four distinct fronds from the same thallus [average surface of a frond: 13.5 cm²
664 (SD = ±7.4)].

665 Physicochemical parameters measurements

666 Temperature, irradiance, pH, salinity and dissolved O₂ level were monitored daily in each
667 aquarium (details in SI). Concentrations of nitrates (NO₃⁻), orthophosphates (PO₄³⁻), and silicates
668 [Si(OH)₄] were determined in field and aquarium seawater at each sampling time (details in SI).
669 Measurement methods were done as described in Briand et al., 2017.

670 Physiological assessment

671 Before extraction procedures, the maximum quantum yield (F_v/F_m) of photosynthetic energy
672 conversion of the photosystem II (PSII) of each sample was measured using a pulse-amplitude
673 modulated chlorophyll fluorometer (JUNIOR-PAM teaching Chlorophyll Fluorometer, Walz,
674 Germany). A frond of each replicate was kept 2 min in the dark and three measures were done
675 by placing directly the optic fiber along three surface areas chosen haphazardly on the algal frond.
676 The mannitol being a main primary source of energy for brown seaweeds, its concentration can
677 be used as a proxy linked with CO₂ fixation through the seaweed photosynthesis (Saha et al.,
678 2014). The relative concentration of this primary metabolite was determined through the
679 metabolomics analysis (see below). The algal growth was investigated throughout the experiment
680 by measuring the length of all thalli sampled for the cytometry, metabolomics and metabarcoding
681 experiments, and then kept in the herbarium. Furthermore, a particular attention was paid during
682 the whole experiment to identify any visual evidence of thallus deteriorations such as bleaching
683 or other types of tissue degradation.

684 Flow cytometry analyses

685 Flow cytometry (FCM) analyses were used to assess the densities of heterotrophic prokaryotes at
686 the surface of the algal samples. Epiphytic cells were collected by scraping the surface of an entire
687 frond of each sample with a sterile scalpel, prefiltered using 40 μm cell strainers, fixed in 4 mL of

688 1% glutaraldehyde filtered seawater solution and conserved at -80°C. The other fronds of each
689 thalli samples were kept for metabarcoding and metabolomics analyses. Aggregated cells were
690 dissociated with an optimized sonication time of 2 min. Samples were centrifugated at 800g for
691 1 min and 200 µL of supernatant were stained using SYBR Green I (Invitrogen, Carlsbad, CA, USA).
692 Cells were enumerated using a BD Accuri C6 flow cytometer (BD Biosciences, San Jose, CA, USA)
693 as previously described (Paix et al., 2020). Results were expressed as densities of cells (cells.cm⁻²)
694 using the measured surface area of each algal sample.

695 16S rRNA gene metabarcoding analyses

696 Epiphytic cells were collected by scraping the surface of an entire frond of each sample with a
697 sterile scalpel. DNA extraction was performed using the DNeasy PowerBiofilm kit (MoBio, Qiagen,
698 Germantown, MD, USA) and samples were conserved at -80°C (Paix et al., 2019, 2020).

699 The NOCHL primers were previously designed specifically to minimize the contamination from
700 plastid 16S rRNA gene (Thomas et al., 2020). At first, they were tested to estimate their efficiency
701 to avoid amplification of chloroplastic 16S rRNA gene and were compared to the 515F-Y/926R
702 primers sets (Parada et al., 2016). Both pairs of primers were tested on triplicates of t₀ and t₁
703 (AT/AI) samples. The treatment of sequences for these analyses with both primers pairs was
704 performed as described below.

705 Following these analyses, 16S rRNA genes of all samples were amplified using the NOCHL primers.
706 Amplicons were sent to Eurofins Genomics (Ebersberg, Germany) for MiSeq Illumina sequencing
707 (2 × 300 bp). 16S rRNA gene reads were processed using the FROGS workflow under the Galaxy
708 environment (Escudié et al., 2018). Clustering step for generating operational taxonomic units
709 (OTUs) was performed using SWARM with a clustering aggregation distance set to 3 (Mahé et al.,
710 2014). Chimeric sequences were *de novo* removed using VSEARCH (Rognes et al., 2016). OTUs
711 representing less than 0.005% of all the sequences were removed. OTUs were affiliated with the
712 silva132 16S rRNA gene database. The final matrix was obtained by performing a rarefaction to
713 the minimum library size (21 642 reads) using the “phyloseq” R package (McMurdie and Holmes,
714 2013).

715 α -diversity was estimated using Chao1 and Shannon indexes. β -diversity was analyzed with a non-
716 metric multidimensional scaling (NMDS) using weighted UniFrac distances allowing to consider
717 phylogenetic relationships between OTUs. These analyses were performed using the “phyloseq”
718 R package and graphical outputs were generated using the “ggplot2” R package.

719 A Venn diagram was constructed to reveal percentages of OTUs and sequences shared between
720 the samples collected at different sampling times. An OTU was considered as common to all the
721 sampling times when it was found a least in one replicate of each sampling time. The Venn
722 diagram was calculated with the Venn webtool
723 (<http://bioinformatics.psb.ugent.be/webtools/Venn/>). LEfSe analyses were conducted to reveal
724 discriminant taxa whether specific to a sampling time (from field to t_3 samples) or a particular
725 controlled cross-condition ($n = 9$). LEfSe analyses were performed under the Galaxy environment
726 with a LDA threshold set to 3.4. A focus on specific comparisons was made with SIMPER analyses
727 to reveal the main contributing genera involved in the dissimilarity between field and t_0 samples.
728 SIMPER analyses were conducted with the “vegan” R package with p values calculated through
729 999 permutations.

730 UHPLC metabolomics analyses

731 Extraction of surface metabolites and sample preparation were performed as described in Paix et
732 al., 2019, 2020 (details in SI), using an entire frond of each sample. Surface extracts were analyzed
733 using a UHPLC-ESI-HRMS system (Dionex Ultimate 3000 rapid Separation; Thermo Fisher
734 Scientific) equipped with an analytical core-shell reversed phase column (150×2.1 mm, $1.7 \mu\text{m}$,
735 Kinetex Phenyl-Hexyl; Phenomenex, Le Pecq, France) and coupled with an ESI-QToF Impact II mass
736 spectrometer (Bruker Daltonics, Bremen, Germany) using a positive ionization mode (details in
737 SI).

738 Raw UPLC-MS data were converted into netCDF files using DataAnalysis software (v. 4.3; Bruker,
739 Germany) and processed for peak finding, integration and alignment using MzMine 2 (version
740 2.53, Pluskal et al., 2010; details in SI). Data were filtered according to Favre et al., 2017, by taking
741 into account signal/noise ratio, coefficient of variation and coefficient of correlation. The resulting
742 data matrix (101 features) was \log_{10} -transformed, mean-centered, normalized using the sum of

743 the chromatographic peak areas according to Paix et al., 2020. The data matrix was then analyzed
744 using principal component analysis (PCA) and partial least-square discriminant analysis (PLS-DA)
745 to determine the chemical biomarkers of a specific condition of temperature and irradiance.

746 The global annotation was performed as described in Paix et al., 2019, 2020; Carriot et al., 2020.
747 Briefly, the annotation was based on the use of an “in-house” database described in Carriot et al.,
748 2021, gathering metabolites annotated through the use of molecular networks (details in SI).
749 Based on the PLS-DA components, VIP scores were calculated and indicated the importance of
750 each m/z feature in the discrimination between each group of samples, allowing then to identify
751 the main biomarkers of a specific condition of temperature and irradiance. A particular attention
752 was paid on compounds with a VIP score above 0.6 (details in SI). Thus, among the 101 features
753 of the data matrix, the 30 metabolites with the highest VIP scores were annotated. In brief,
754 annotation was assessed by comparison of MS/MS spectra with those of our in-house database
755 (purified compounds and commercial standards listed in SI), and public databases such as MetLin,
756 MoNA or Lipidmaps. To confirm the annotation, elucidation of the MS/MS fragmentation
757 pathway was performed and when possible compared to the literature (details in SI).

758 **Statistical tests**

759 Three-way ANOVA tests were conducted to assess the significance of physicochemical
760 parameters, PAM measures, metabolites, densities, according to each experimental condition
761 (time, irradiance and temperature). ANOVA tests were followed by pairwise multiple comparison
762 tests. Tukey’s post-hoc tests were performed for PAM measures, discriminant metabolites,
763 densities and α -diversity metrics. Duncan test with Benjamini-Hochberg method for p -value
764 correction was performed as a multiple testing method to evaluate differences between groups
765 for discriminant taxa. Following NMDS and PCA, overall differences between
766 temperature/irradiance conditions were statistically tested with PERMANOVA and followed by a
767 multivariate pairwise test. These analyses were conducted on R with “ade4”, “agricolae”, “vegan”
768 and “RVAideMemoire” packages. PLS-DA were subjected to cross validations using
769 MetaboAnalyst 4.0 (<https://www.metaboanalyst.ca>).

770

771 Acknowledgments

772 This work was supported by the “Sud Provence-Alpes-Côte d’Azur” regional council (B.P. PhD
773 grant). This work was also carried out with infrastructure provided by EMBRC France (grant no.
774 ANR-10-INBS-0002) project “EMPREINTES”. We are grateful to N. Carriot (MAPIEM, University of
775 Toulon, France) for his help with annotation of the metabolomics data processing, to S. Greff
776 (IMBE, Aix-Marseille University, France), to C. Leroux (Corsaire-Metabomer, FR 2424, Marine
777 Station, France) and E. Bourrigaux (Visiting scientist facilities service, FR 2424, Roscoff Marine
778 Station, France) for their technical supports. We acknowledge F. Thomas and A. Gobet for sharing
779 their useful work on the NOCHL primers. We thank C. Vieira for confirming the identification of
780 *Taonia atomaria* through phylogenetic analyses.

781

782 Data accessibility

783 Sequences data were deposited and are publicly available in the NCBI Sequences Read Archive
784 (SRA) under the BioProject ID PRJNA684487 accession number. Raw data for LC-ESI-(+)-MS/MS
785 experiments were deposited and are publicly available in the MassIVE platform under the ID
786 MSV000084512, respectively.

787

788 Author contributions

789 BP, GC, JFB, CL and PP designed the study. BP and PP performed field sampling. BP and GS
790 designed and constructed the whole experimental devices. BP performed the controlled
791 conditions experiments, PAM measurements, metabolomics and metabarcoding experiments. BP
792 and BM performed cytometry analyses. NL and CLP performed chemical analyses of seawater
793 samples. BP, GC, JFB, PP and CL analyzed all the data. All authors participated to the writing of
794 the manuscript.

795

796 **References**

- 797 Akagawa-Matsushita, M., Matsuo, M., Koga, Y., and Yamasato, K. (1992). *Alteromonas atlantica*
798 sp. nov. and *Alteromonas carrageenovora* sp. nov., bacteria that decompose algal
799 polysaccharides. *Int. J. Syst. Evol. Microbiol.* 42, 621–627. doi:10.1099/00207713-42-4-
800 621.
- 801 Barbeyron, T., L’Haridon, S., Corre, E., Kloareg, B., and Potin, P. (2001). *Zobellia galactanovorans*
802 gen. nov., sp. nov., a marine species of Flavobacteriaceae isolated from a red alga, and
803 classification of [*Cytophaga*] *uliginosa* (ZoBell and Upham 1944) Reichenbach 1989 as
804 *Zobellia uliginosa* gen. nov., comb. nov. *Int. J. Syst. Evol. Microbiol.* 51, 985–997.
805 doi:10.1099/00207713-51-3-985.
- 806 Barbeyron, T., Thomas, F., Barbe, V., Teeling, H., Schenowitz, C., Dossat, C., et al. (2016). Habitat
807 and taxon as driving forces of carbohydrate catabolism in marine heterotrophic bacteria:
808 example of the model algae-associated bacterium *Zobellia galactanivorans* DsijT. *Environ.*
809 *Microbiol.* 18, 4610–4627. doi:10.1111/1462-2920.13584.
- 810 Bech, P. K., Schultz-Johansen, M., Glaring, M. A., Barbeyron, T., Czjzek, M., and Stougaard, P.
811 (2017). *Paraglaciecola hydrolytica* sp. nov., a bacterium with hydrolytic activity against
812 multiple seaweed-derived polysaccharides. *Int. J. Syst. Evol. Microbiol.* 67, 2242–2247.
813 doi:10.1099/ijsem.0.001933.
- 814 Bindoff, N. L., Cheung, W. W. L., Kairo, J. G., Arístegui, J., Guinder, V. A., Hallberg, R., et al. (2019).
815 “Chapter 5: Changing ocean, marine ecosystems, and dependent communities,” in *IPCC*
816 *Special Report on the Ocean and Cryosphere in a Changing Climate*.
- 817 Bokulich, N. A., Subramanian, S., Faith, J. J., Gevers, D., Gordon, J. I., Knight, R., et al. (2013).
818 Quality-filtering vastly improves diversity estimates from Illumina amplicon sequencing.
819 *Nat. Methods* 10, 57–59. doi:10.1038/nmeth.2276.
- 820 Briand, J.-F., Barani, A., Garnier, C., Réhel, K., Urvois, F., LePoupon, C., et al. (2017). Spatio-
821 temporal variations of marine biofilm communities colonizing artificial substrata including
822 antifouling coatings in contrasted french coastal environments. *Microb. Ecol.* 74, 585–598.
823 doi:10.1007/s00248-017-0966-2.
- 824 Bullock, H. A., Luo, H., and Whitman, W. B. (2017). Evolution of dimethylsulfoniopropionate
825 metabolism in marine phytoplankton and bacteria. *Front. Microbiol.* 8, 637.
826 doi:10.3389/fmicb.2017.00637.
- 827 Campbell, A. H., Harder, T., Nielsen, S., Kjelleberg, S., and Steinberg, P. D. (2011). Climate change
828 and disease: bleaching of a chemically defended seaweed. *Glob. Change Biol.* 17, 2958–
829 2970. doi:10.1111/j.1365-2486.2011.02456.x.

- 830 Campbell, A. H., Vergés, A., and Steinberg, P. D. (2014). Demographic consequences of disease in
831 a habitat-forming seaweed and impacts on interactions between natural enemies. *Ecology*
832 95, 142–152.
- 833 Carriot, N., Paix, B., Greff, S., Viguier, B., Briand, J.-F., and Culioli, G. (2021). Integration of LC/MS-
834 based molecular networking and classical phytochemical approach allows in-depth
835 annotation of the metabolome of non-model organisms - The case study of the brown
836 seaweed *Taonia atomaria*. *Talanta* 225, 121925. doi:10.1016/j.talanta.2020.121925.
- 837 Case, R. J., Longford, S. R., Campbell, A. H., Low, A., Tujula, N., Steinberg, P. D., et al. (2011).
838 Temperature induced bacterial virulence and bleaching disease in a chemically defended
839 marine macroalga. *Environ. Microbiol.* 13, 529–537. doi:10.1111/j.1462-
840 2920.2010.02356.x.
- 841 Collins, M., Knutti, R., Arblaster, J., Dufresne, J.-L., Fichet, T., Friedlingstein, P., et al. (2013).
842 “Chapter 12: Long-term climate change: Projections, commitments and irreversibility,” in
843 *IPCC, 2013: Climate Change 2013: The Physical Science Basis. Contribution of Working*
844 *Group I to the Fifth Assessment Report of the Intergovernmental Panel on Climate Change.*
- 845 Cram, J. A., Parada, A. E., and Fuhrman, J. A. (2016). Dilution reveals how viral lysis and grazing
846 shape microbial communities. *Limnol. Oceanogr.* 61, 889–905.
847 doi:https://doi.org/10.1002/lno.10259.
- 848 Curson, A. R. J., Rogers, R., Todd, J. D., Brearley, C. A., and Johnston, A. W. B. (2008). Molecular
849 genetic analysis of a dimethylsulfonylpropionate lyase that liberates the climate-changing
850 gas dimethylsulfide in several marine alpha-proteobacteria and *Rhodobacter sphaeroides*.
851 *Environ. Microbiol.* 10, 757–767. doi:10.1111/j.1462-2920.2007.01499.x.
- 852 Curson, A. R. J., Todd, J. D., Sullivan, M. J., and Johnston, A. W. B. (2011). Catabolism of
853 dimethylsulfonylpropionate: microorganisms, enzymes and genes. *Nat. Rev. Microbiol.*
854 9, 849–859. doi:10.1038/nrmicro2653.
- 855 Dittami, S. M., Eveillard, D., and Tonon, T. (2014). A metabolic approach to study algal–bacterial
856 interactions in changing environments. *Mol. Ecol.* 23, 1656–1660.
857 doi:10.1111/mec.12670.
- 858 Dogs, M., Wemheuer, B., Wolter, L., Bergen, N., Daniel, R., Simon, M., et al. (2017).
859 Rhodobacteraceae on the marine brown alga *Fucus spiralis* are predominant and show
860 physiological adaptation to an epiphytic lifestyle. *Syst. Appl. Microbiol.* 40, 370–382.
861 doi:10.1016/j.syapm.2017.05.006.
- 862 Egan, S., Fernandes, N. D., Kumar, V., Gardiner, M., and Thomas, T. (2014). Bacterial pathogens,
863 virulence mechanism and host defence in marine macroalgae. *Environ. Microbiol.* 16, 925–
864 938. doi:10.1111/1462-2920.12288.

- 865 Egan, S., and Gardiner, M. (2016). Microbial dysbiosis: rethinking disease in marine ecosystems.
866 *Front. Microbiol.* 7, 991. doi:10.3389/fmicb.2016.00991.
- 867 Egan, S., Harder, T., Burke, C., Steinberg, P., Kjelleberg, S., and Thomas, T. (2013). The seaweed
868 holobiont: understanding seaweed–bacteria interactions. *FEMS Microbiol. Rev.* 37, 462–
869 476. doi:10.1111/1574-6976.12011.
- 870 Eggert, A. (2012). “Seaweed responses to temperature,” in *Seaweed Biology: Novel Insights into*
871 *Ecophysiology, Ecology and Utilization Ecological Studies.*, eds. C. Wiencke and K. Bischof
872 (Berlin, Heidelberg: Springer), 47–66. doi:10.1007/978-3-642-28451-9_3.
- 873 Escudié, F., Auer, L., Bernard, M., Mariadassou, M., Cauquil, L., Vidal, K., et al. (2018). FROGS: Find,
874 Rapidly, OTUs with Galaxy Solution. *Bioinformatics* 34, 1287–1294.
875 doi:10.1093/bioinformatics/btx791.
- 876 Favre, L., Ortalo-Magné, A., Greff, S., Pérez, T., Thomas, O. P., Martin, J.-C., et al. (2017).
877 Discrimination of four marine biofilm-forming bacteria by LC-MS metabolomics and
878 influence of culture parameters. *J. Proteome Res.* 16, 1962–1975.
879 doi:10.1021/acs.jproteome.6b01027.
- 880 Fernandes, N., Case, R. J., Longford, S. R., Seyedsayamdost, M. R., Steinberg, P. D., Kjelleberg, S.,
881 et al. (2011). Genomes and virulence factors of novel bacterial pathogens causing
882 bleaching disease in the marine red alga *Delisea pulchra*. *PLoS One* 6, e27387.
883 doi:10.1371/journal.pone.0027387.
- 884 Florez, J. Z., Camus, C., Hengst, M. B., Marchant, F., and Buschmann, A. H. (2019). Structure of the
885 epiphytic bacterial communities of *Macrocystis pyrifera* in localities with contrasting
886 nitrogen concentrations and temperature. *Algal Res.* 44, 101706.
887 doi:10.1016/j.algal.2019.101706.
- 888 Forster, R. M., and Dring, M. J. (1994). Influence of blue light on the photosynthetic capacity of
889 marine plants from different taxonomic, ecological and morphological groups. *European*
890 *Journal of Phycology* 29, 21–27. doi:10.1080/09670269400650441.
- 891 Fuchs, B. M., Spring, S., Teeling, H., Quast, C., Wulf, J., Schattenhofer, M., et al. (2007).
892 Characterization of a marine gammaproteobacterium capable of aerobic anoxygenic
893 photosynthesis. *Proc Natl Acad Sci U S A* 104, 2891–2896. doi:10.1073/pnas.0608046104.
- 894 Gardiner, M., Bournazos, A. M., Maturana-Martinez, C., Zhong, L., and Egan, S. (2017).
895 Exoproteome analysis of the seaweed pathogen *Nautella italica* R11 reveals temperature-
896 dependent regulation of RTX-like proteins. *Front. Microbiol.* 8.
897 doi:10.3389/fmicb.2017.01203.
- 898 Ghaderiardakani, F., Califano, G., Mohr, J. F., Abreu, M. H., Coates, J. C., and Wichard, T. (2019).
899 Analysis of algal growth- and morphogenesis-promoting factors in an integrated multi-

- 900 trophic aquaculture system for farming *Ulva* spp. *Aquac. Environ. Interact.* 11, 375–391.
901 doi:10.3354/aei00319.
- 902 Ghaderiardakani, F., Coates, J. C., and Wichard, T. (2017). Bacteria-induced morphogenesis of
903 *Ulva intestinalis* and *Ulva mutabilis* (Chlorophyta): a contribution to the lottery theory.
904 *FEMS Microbiol. Ecol.* 93. doi:10.1093/femsec/fix094.
- 905 Gobet, A., Barbeyron, T., Matard-Mann, M., Magdelenat, G., Vallenet, D., Duchaud, E., et al.
906 (2018). Evolutionary evidence of algal polysaccharide degradation acquisition by
907 *Pseudoalteromonas carrageenovora* 9T to adapt to macroalgal niches. *Front. Microbiol.* 9,
908 2740. doi:10.3389/fmicb.2018.02740.
- 909 Groisillier, A., Labourel, A., Michel, G., and Tonon, T. (2015). The mannitol utilization system of
910 the marine bacterium *Zobellia galactanivorans*. *Appl. Environ. Microbiol.* 81, 1799–1812.
911 doi:10.1128/AEM.02808-14.
- 912 Grosser, K., Zedler, L., Schmitt, M., Dietzek, B., Popp, J., and Pohnert, G. (2012). Disruption-free
913 imaging by Raman spectroscopy reveals a chemical sphere with antifouling metabolites
914 around macroalgae. *Biofouling* 28, 687–696. doi:10.1080/08927014.2012.700306.
- 915 Guiry, M. D., and Guiry, M. D. (2020). *AlgaeBase*. World-wide electronic publication, National
916 University of Ireland, Galway. <https://www.algaebase.org>; searched on 05 June 2020.
- 917 Hanelt, D., Uhrmacher, S., and Nultsch, W. (1995). The effect of photoinhibition on photosynthetic
918 oxygen production in the brown alga *Dictyota dichotoma*. *Botanica Acta* 108, 99–105.
919 doi:10.1111/j.1438-8677.1995.tb00838.x.
- 920 Harder, T., Campbell, A. H., Egan, S., and Steinberg, P. D. (2012). Chemical mediation of ternary
921 interactions between marine holobionts and their environment as exemplified by the red
922 alga *Delisea pulchra*. *J. Chem. Ecol.* 38, 442–450. doi:10.1007/s10886-012-0119-5.
- 923 Hartmann, A., Albert, A., and Ganzera, M. (2015). Effects of elevated ultraviolet radiation on
924 primary metabolites in selected alpine algae and cyanobacteria. *J. Photochem. Photobiol.*
925 *B* 149, 149–155. doi:10.1016/j.jphotobiol.2015.05.016.
- 926 Heo, S.-J., and Jeon, Y.-J. (2009). Protective effect of fucoxanthin isolated from *Sargassum*
927 *siliquastrum* on UV-B induced cell damage. *J. Photochem. Photobiol. B* 95, 101–107.
928 doi:10.1016/j.jphotobiol.2008.11.011.
- 929 Hollants, J., Leliaert, F., De Clerck, O., and Willems, A. (2013). What we can learn from sushi: a
930 review on seaweed-bacterial associations. *FEMS Microbiol. Ecol.* 83, 1–16.
931 doi:10.1111/j.1574-6941.2012.01446.x.
- 932 Howard, E. C., Sun, S., Biers, E. J., and Moran, M. A. (2008). Abundant and diverse bacteria
933 involved in DMSP degradation in marine surface waters. *Environ. Microbiol.* 10, 2397–
934 2410. doi:10.1111/j.1462-2920.2008.01665.x.

- 935 Huggett, M. J., McMahon, K., and Bernasconi, R. (2018). Future warming and acidification result
936 in multiple ecological impacts to a temperate coralline alga. *Environ. Microbiol.* 20, 2769–
937 2782. doi:10.1111/1462-2920.14113.
- 938 Inaba, M., Suzuki, I., Szalontai, B., Kanesaki, Y., Los, D. A., Hayashi, H., et al. (2003). Gene-
939 engineered rigidification of membrane lipids enhances the cold inducibility of gene
940 expression in *Synechocystis*. *J. Biol. Chem.* 278, 12191–12198.
941 doi:10.1074/jbc.M212204200.
- 942 Karsten, U., Kirst, G. O., and Wiencke, C. (1992). Dimethylsulphoniopropionate (DMSP)
943 accumulation in green macroalgae from polar to temperate regions: interactive effects of
944 light versus salinity and light versus temperature. *Polar Biol.* 12, 603–607.
945 doi:10.1007/BF00236983.
- 946 Karsten, U., Wiencke, C., and Kirst, G. O. (1990). The effect of light intensity and daylength on the
947 β -dimethylsulphoniopropionate (DMSP) content of marine green macroalgae from
948 Antarctica. *Plant Cell Environ.* 13, 989–993. doi:10.1111/j.1365-3040.1990.tb01991.x.
- 949 Kessler, R. W., Weiss, A., Kuegler, S., Hermes, C., and Wichard, T. (2018). Macroalgal-bacterial
950 interactions: Role of dimethylsulfonylpropionate in microbial gardening by *Ulva*
951 (Chlorophyta). *Mol. Ecol.* 27, 1808–1819. doi:10.1111/mec.14472.
- 952 Kets, E. P., Galinski, E. A., de Wit, M., de Bont, J. A., and Heipieper, H. J. (1996). Mannitol, a novel
953 bacterial compatible solute in *Pseudomonas putida* S12. *J. Bacteriol.* 178, 6665–6670.
954 doi:10.1128/jb.178.23.6665-6670.1996.
- 955 Koblížek, M. (2015). Ecology of aerobic anoxygenic phototrophs in aquatic environments. *FEMS*
956 *Microbiol. Rev.* 39, 854–870. doi:10.1093/femsre/fuv032.
- 957 Kumar, V., Zozaya-Valdes, E., Kjelleberg, S., Thomas, T., and Egan, S. (2016). Multiple opportunistic
958 pathogens can cause a bleaching disease in the red seaweed *Delisea pulchra*. *Environ.*
959 *Microbiol.* 18, 3962–3975. doi:10.1111/1462-2920.13403.
- 960 Lachnit, T., Fischer, M., Künzel, S., Baines, J. F., and Harder, T. (2013). Compounds associated with
961 algal surfaces mediate epiphytic colonization of the marine macroalga *Fucus vesiculosus*.
962 *FEMS Microbiol. Ecol.* 84, 411–420. doi:10.1111/1574-6941.12071.
- 963 Lachnit, T., Wahl, M., and Harder, T. (2010). Isolated thallus-associated compounds from the
964 macroalga *Fucus vesiculosus* mediate bacterial surface colonization in the field similar to
965 that on the natural alga. *Biofouling* 26, 247–255. doi:10.1080/08927010903474189.
- 966 Lawes, J. C., Neilan, B. A., Brown, M. V., Clark, G. F., and Johnston, E. L. (2016). Elevated nutrients
967 change bacterial community composition and connectivity: high throughput sequencing
968 of young marine biofilms. *Biofouling* 32, 57–69. doi:10.1080/08927014.2015.1126581.

- 969 Lehvo, A., Bäck, S., and Kiirikki, M. (2001). Growth of *Fucus vesiculosus* L. (Phaeophyta) in the
970 Northern Baltic proper: Energy and nitrogen storage in seasonal environment. *Botanica*
971 *Marina* 44, 345–350. doi:10.1515/BOT.2001.044.
- 972 Longford, S. R., Campbell, A. H., Nielsen, S., Case, R. J., Kjelleberg, S., and Steinberg, P. D. (2019).
973 Interactions within the microbiome alter microbial interactions with host chemical
974 defences and affect disease in a marine holobiont. *Sci. Rep.* 9, 1363. doi:10.1038/s41598-
975 018-37062-z.
- 976 Loreau, M., Naeem, S., Inchausti, P., Bengtsson, J., Grime, J. P., Hector, A., et al. (2001).
977 Biodiversity and ecosystem functioning: current knowledge and future challenges. *Science*
978 294, 804–808. doi:10.1126/science.1064088.
- 979 Los, D. A., and Murata, N. (2004). Membrane fluidity and its roles in the perception of
980 environmental signals. *Biochim. Biophys. Acta* 1666, 142–157.
981 doi:10.1016/j.bbamem.2004.08.002.
- 982 Lyons, D. A., Scheibling, R. E., and Alstyne, K. L. V. (2010). Spatial and temporal variation in DMSP
983 content in the invasive seaweed *Codium fragile* ssp. *fragile*: effects of temperature, light
984 and grazing. *Mar. Ecol. Prog. Ser.* 417, 51–61. doi:10.3354/meps08818.
- 985 Mahé, F., Rognes, T., Quince, C., Vargas, C. de, and Dunthorn, M. (2014). Swarm: robust and fast
986 clustering method for amplicon-based studies. *PeerJ* 2, e593. doi:10.7717/peerj.593.
- 987 Martin, S., Castets, M.-D., and Clavier, J. (2006). Primary production, respiration and calcification
988 of the temperate free-living coralline alga *Lithothamnion corallioides*. *Aquat. Bot.* 85, 121–
989 128. doi:10.1016/j.aquabot.2006.02.005.
- 990 Maximilien, R., Nys, R. de, Holmström, C., Gram, L., Givskov, M., Crass, K., et al. (1998). Chemical
991 mediation of bacterial surface colonisation by secondary metabolites from the red alga
992 *Delisea pulchra*. *Aquat. Microb. Ecol.* 15, 233–246. doi:10.3354/ame015233.
- 993 McMurdie, P. J., and Holmes, S. (2013). phyloseq: an R package for reproducible interactive
994 analysis and graphics of microbiome census data. *PLoS One* 8, e61217.
995 doi:10.1371/journal.pone.0061217.
- 996 Mensch, B., Neulinger, S. C., Graiff, A., Pansch, A., Künzel, S., Fischer, M. A., et al. (2016).
997 Restructuring of epibacterial communities on *Fucus vesiculosus* forma *mytili* in response
998 to elevated pCO₂ and increased temperature levels. *Front. Microbiol.* 7, 434.
999 doi:10.3389/fmicb.2016.00434.
- 1000 Minich, J. J., Morris, M. M., Brown, M., Doane, M., Edwards, M. S., Michael, T. P., et al. (2018).
1001 Elevated temperature drives kelp microbiome dysbiosis, while elevated carbon dioxide
1002 induces water microbiome disruption. *PLoS One* 13, e0192772.
1003 doi:10.1371/journal.pone.0192772.

- 1004 Moore, P. D. (2005). Roots of stability. *Nature* 437, 959–961. doi:10.1038/437959a.
- 1005 Mou, X., Moran, M. A., Stepanauskas, R., González, J. M., and Hodson, R. E. (2005). Flow-
1006 cytometric cell sorting and subsequent molecular analyses for culture-independent
1007 identification of bacterioplankton involved in dimethylsulfoniopropionate
1008 transformations. *Appl. Environ. Microbiol.* 71, 1405–1416. doi:10.1128/AEM.71.3.1405-
1009 1416.2005.
- 1010 Murakami, H., Serisawa, Y., Kurashima, A., and Yokohama, Y. (2004). Photosynthetic
1011 performances of temperate *Sargassum* and Kelp species growing in the same habitat.
1012 *Algae* 19, 207–216.
- 1013 Othmani, A., Briand, J.-F., Ayé, M., Molmeret, M., and Culioli, G. (2016). Surface metabolites of
1014 the brown alga *Taonia atomaria* have the ability to regulate epibiosis. *Biofouling* 32, 801–
1015 813. doi:10.1080/08927014.2016.1198954.
- 1016 Paix, B., Carriot, N., Barry-Martin, R., Greff, S., Misson, B., Briand, J.-F., et al. (2020). A multi-
1017 omics analysis suggests links between the differentiated surface metabolome and
1018 epiphytic microbiota along the thallus of a Mediterranean seaweed holobiont. *Front.*
1019 *Microbiol.* 11, 494. doi:10.3389/fmicb.2020.00494.
- 1020 Paix, B., Layglon, N., Le Poupon, C., D’Onofrio, S., Misson, B., Garnier, C., et al. (submitted). A
1021 multi-omics approach deciphers how temperature and copper stress shape seaweed-
1022 microbiota interactions at the surface of *Taonia atomaria* on the NW Mediterranean
1023 coast. *Submitted to Microbiome*.
- 1024 Paix, B., Othmani, A., Debroas, D., Culioli, G., and Briand, J.-F. (2019). Temporal covariation of
1025 epibacterial community and surface metabolome in the Mediterranean seaweed
1026 holobiont *Taonia atomaria*. *Environ. Microbiol.* 21, 3346–3363. doi:10.1111/1462-
1027 2920.14617.
- 1028 Parada, A. E., Needham, D. M., and Fuhrman, J. A. (2016). Every base matters: assessing small
1029 subunit rRNA primers for marine microbiomes with mock communities, time series and
1030 global field samples. *Environ. Microbiol.* 18, 1403–1414. doi:10.1111/1462-2920.13023.
- 1031 Perez-Bermudez, P., Garcia-Carrascosa, M., Cornejo, M. J., and Segura, J. (1981). Water-depth
1032 effects in photosynthetic pigment content of the benthic algae *Dictyota dichotoma* and
1033 *Udotea petiolata*. *Aquat. Bot.* 11, 373–377. doi:10.1016/0304-3770(81)90070-X.
- 1034 Pitlik, S. D., and Koren, O. (2017). How holobionts get sick-toward a unifying scheme of disease.
1035 *Microbiome* 5, 64. doi:10.1186/s40168-017-0281-7.
- 1036 Pujalte, M. J., Lucena, T., Ruvira, M. A., Arahal, D. R., and Macián, M. C. (2014). “The family
1037 Rhodobacteraceae,” in *The Prokaryotes: Alphaproteobacteria and Betaproteobacteria*,
1038 eds. E. Rosenberg, E. F. DeLong, S. Lory, E. Stackebrandt, and F. Thompson (Berlin,
1039 Heidelberg: Springer), 439–512. doi:10.1007/978-3-642-30197-1_377.

- 1040 Qiu, Z., Coleman, M. A., Provost, E., Campbell, A. H., Kelaher, B. P., Dalton, S. J., et al. (2019).
1041 Future climate change is predicted to affect the microbiome and condition of habitat-
1042 forming kelp. *Proc. Biol. Sci.* 286, 20181887. doi:10.1098/rspb.2018.1887.
- 1043 Ramus, J., Lemons, F., and Zimmerman, C. (1977). Adaptation of light-harvesting pigments to
1044 downwelling light and the consequent photosynthetic performance of the eulittoral
1045 rockweeds *Ascophyllum nodosum* and *Fucus vesiculosus*. *Mar. Biol.* 42, 293–303.
1046 doi:10.1007/BF00402191.
- 1047 Roberts, E. M., Bowers, D. G., and Davies, A. J. (2018). Tidal modulation of seabed light and its
1048 implications for benthic algae. *Limnology and Oceanography* 63, 91–106.
1049 doi:10.1002/lno.10616.
- 1050 Rognes, T., Flouri, T., Nichols, B., Quince, C., and Mahé, F. (2016). VSEARCH: a versatile open
1051 source tool for metagenomics. *PeerJ* 4, e2584. doi:10.7717/peerj.2584.
- 1052 Romera-Castillo, C., Sarmiento, H., Alvarez-Salgado, X. A., Gasol, J. M., and Marrasé, C. (2011). Net
1053 production and consumption of fluorescent colored dissolved organic matter by natural
1054 bacterial assemblages growing on marine phytoplankton exudates. *Appl. Environ.
1055 Microbiol.* 77, 7490–7498. doi:10.1128/AEM.00200-11.
- 1056 Roth-Schulze, A. J., Pintado, J., Zozaya-Valdés, E., Cremades, J., Ruiz, P., Kjelleberg, S., et al. (2018).
1057 Functional biogeography and host specificity of bacterial communities associated with the
1058 Marine Green Alga *Ulva* spp. *Mol. Ecol.* 27, 1952–1965. doi:10.1111/mec.14529.
- 1059 Rousvoal, S., Groisillier, A., Dittami, S. M., Michel, G., Boyen, C., and Tonon, T. (2011). Mannitol-
1060 1-phosphate dehydrogenase activity in *Ectocarpus siliculosus*, a key role for mannitol
1061 synthesis in brown algae. *Planta* 233, 261–273. doi:10.1007/s00425-010-1295-6.
- 1062 Saha, M., Rempt, M., Grosser, K., Pohnert, G., and Weinberger, F. (2011). Surface-associated
1063 fucoxanthin mediates settlement of bacterial epiphytes on the rockweed *Fucus
1064 vesiculosus*. *Biofouling* 27, 423–433. doi:10.1080/08927014.2011.580841.
- 1065 Saha, M., Rempt, M., Stratil, S. B., Wahl, M., Pohnert, G., and Weinberger, F. (2014). Defence
1066 chemistry modulation by light and temperature shifts and the resulting effects on
1067 associated epibacteria of *Fucus vesiculosus*. *PLoS One* 9, e105333.
1068 doi:10.1371/journal.pone.0105333.
- 1069 Sand, M., Mingote, A. I., Santos, H., Müller, V., and Averhoff, B. (2013). Mannitol, a compatible
1070 solute synthesized by *Acinetobacter baylyi* in a two-step pathway including a salt-induced
1071 and salt-dependent mannitol-1-phosphate dehydrogenase. *Environ. Microbiol.* 15, 2187–
1072 2197. doi:10.1111/1462-2920.12090.
- 1073 Sato, N., and Murata, N. (1980). Temperature shift-induced responses in lipids in the blue-green
1074 alga, *Anabaena variabilis*: the central role of diacylmonogalactosylglycerol in thermo-
1075 adaptation. *Biochim. Biophys. Acta* 619, 353–366. doi:10.1016/0005-2760(80)90083-1.

- 1076 Sato, N., and Murata, N. (1982). Lipid biosynthesis in the blue-green alga, *Anabaena variabilis*: II.
1077 Fatty acids and lipid molecular species. *Biochim. Biophys. Acta* 710, 279–289.
1078 doi:10.1016/0005-2760(82)90110-2.
- 1079 Schäfer, H., Servais, P., and Muyzer, G. (2000). Successional changes in the genetic diversity of a
1080 marine bacterial assemblage during confinement. *Arch. Microbiol.* 173, 138–145.
1081 doi:10.1007/s002039900121.
- 1082 Schüler, L. M., Schulze, P. S. C., Pereira, H., Barreira, L., León, R., and Varela, J. (2017). Trends and
1083 strategies to enhance triacylglycerols and high-value compounds in microalgae. *Algal Res.*
1084 25, 263–273. doi:10.1016/j.algal.2017.05.025.
- 1085 Schultz-Johansen, M., Glaring, M. A., Bech, P. K., and Stougaard, P. (2016). Draft genome
1086 sequence of a novel marine bacterium, *Paraglaciecola* sp. strain s66, with hydrolytic
1087 activity against seaweed polysaccharides. *Genome Announc.* 4.
1088 doi:10.1128/genomeA.00304-16.
- 1089 Selyanin, V., Hauruseu, D., and Koblížek, M. (2016). The variability of light-harvesting complexes
1090 in aerobic anoxygenic phototrophs. *Photosynth. Res.* 128, 35–43. doi:10.1007/s11120-
1091 015-0197-7.
- 1092 Stratil, S. B., Neulinger, S. C., Knecht, H., Friedrichs, A. K., and Wahl, M. (2013). Temperature-
1093 driven shifts in the epibiotic bacterial community composition of the brown macroalga
1094 *Fucus vesiculosus*. *Microbiologyopen* 2, 338–349. doi:10.1002/mbo3.79.
- 1095 Tada, Y., Taniguchi, A., Nagao, I., Miki, T., Uematsu, M., Tsuda, A., et al. (2011). Differing growth
1096 responses of major phylogenetic groups of marine bacteria to natural phytoplankton
1097 blooms in the western North Pacific Ocean. *Appl. Environ. Microbiol.* 77, 4055–4065.
1098 doi:10.1128/AEM.02952-10.
- 1099 Ternon, E., Paix, B., Thomas, O. P., Briand, J.-F., and Culioli, G. (2020). Exploring the role of
1100 macroalgal surface metabolites on the settlement of the benthic dinoflagellate *Ostreopsis*
1101 cf. *ovata*. *Front. Mar. Sci.* 7. doi:10.3389/fmars.2020.00683.
- 1102 Thomas, F., Barbeyron, T., Tonon, T., Génicot, S., Czjzek, M., and Michel, G. (2012).
1103 Characterization of the first alginolytic operons in a marine bacterium: from their
1104 emergence in marine Flavobacteriia to their independent transfers to marine
1105 Proteobacteria and human gut Bacteroides. *Environ. Microbiol.* 14, 2379–2394.
1106 doi:10.1111/j.1462-2920.2012.02751.x.
- 1107 Thomas, F., Dittami, S. M., Brunet, M., Duff, N. L., Tanguy, G., Leblanc, C., et al. (2020). Evaluation
1108 of a new primer combination to minimize plastid contamination in 16S rDNA
1109 metabarcoding analyses of alga-associated bacterial communities. *Environ. Microbiol.*
1110 *Rep.* 12, 30–37. doi:10.1111/1758-2229.12806.

- 1111 Thomas, F., Lundqvist, L. C. E., Jam, M., Jeudy, A., Barbeyron, T., Sandström, C., et al. (2013).
1112 Comparative characterization of two marine alginate lyases from *Zobellia galactanivorans*
1113 reveals distinct modes of action and exquisite adaptation to their natural substrate. *J. Biol.*
1114 *Chem.* 288, 23021–23037. doi:10.1074/jbc.M113.467217.
- 1115 Van Alstyne, K. L., and Puglisi, M. P. (2007). DMSP in marine macroalgae and macroinvertebrates:
1116 Distribution, function, and ecological impacts. *Aquat. Sci.* 69, 394–402.
1117 doi:10.1007/s00027-007-0888-z.
- 1118 van der Loos, L. M., Eriksson, B. K., and Falcão Salles, J. (2019). The macroalgal holobiont in a
1119 changing sea. *Trends Microbiol.* 27, 635–650. doi:10.1016/j.tim.2019.03.002.
- 1120 Viano, Y., Bonhomme, D., Camps, M., Briand, J.-F., Ortalo-Magné, A., Blache, Y., et al. (2009).
1121 Diterpenoids from the Mediterranean brown alga *Dictyota* sp. evaluated as antifouling
1122 substances against a marine bacterial biofilm. *J. Nat. Prod.* 72, 1299–1304.
1123 doi:10.1021/np900102f.
- 1124 Wahl, M., Goecke, F., Labes, A., Dobretsov, S., and Weinberger, F. (2012). The second skin:
1125 ecological role of epibiotic biofilms on marine organisms. *Front. Microbiol.* 3, 292.
1126 doi:10.3389/fmicb.2012.00292.
- 1127 Webster, N. S., Soo, R., Cobb, R., and Negri, A. P. (2011). Elevated seawater temperature causes
1128 a microbial shift on crustose coralline algae with implications for the recruitment of coral
1129 larvae. *ISME J.* 5, 759–770. doi:10.1038/ismej.2010.152.
- 1130 Weinberger, F., Rohde, S., Oschmann, Y., Shahnaz, L., Dobretsov, S., and Wahl, M. (2011). Effects
1131 of limitation stress and of disruptive stress on induced antigrazing defense in the bladder
1132 wrack *Fucus vesiculosus*. *Mar. Ecol. Prog. Ser.* 427, 83–94. doi:10.3354/meps09044.
- 1133 Wichard, T., and Beemelmanns, C. (2018). Role of chemical mediators in aquatic interactions
1134 across the Prokaryote-Eukaryote boundary. *J. Chem. Ecol.* 44, 1008–1021.
1135 doi:10.1007/s10886-018-1004-7.
- 1136 Wichard, T., Charrier, B., Mineur, F., Bothwell, J. H., Clerck, O. D., and Coates, J. C. (2015). The
1137 green seaweed *Ulva*: a model system to study morphogenesis. *Front. Plant Sci.* 6, 72.
1138 doi:10.3389/fpls.2015.00072.
- 1139 Wietz, M., Duncan, K., Patin, N. V., and Jensen, P. R. (2013). Antagonistic interactions mediated
1140 by marine bacteria: the role of small molecules. *J Chem Ecol* 39, 879–891.
1141 doi:10.1007/s10886-013-0316-x.
- 1142 Yoon, J.-H., Kang, S.-J., Park, S., Oh, K.-H., and Oh, T.-K. (2010). *Jannaschia seohaensis* sp. nov.,
1143 isolated from a tidal flat sediment. *Int. J. Syst. Evol. Microbiol.* 60, 191–195.
1144 doi:10.1099/ij.s.0.011270-0.

- 1145 Zahid, N., Schweiger, P., Galinski, E., and Deppenmeier, U. (2015). Identification of mannitol as
1146 compatible solute in *Gluconobacter oxydans*. *Appl. Microbiol. Biotechnol.* 99, 5511–5521.
1147 doi:10.1007/s00253-015-6626-x.
- 1148 Zemb, O., West, N., Bourrain, M., Godon, J. J., and Lebaron, P. (2010). Effect of a transient
1149 perturbation on marine bacterial communities with contrasting history. *J. Appl. Microbiol.*
1150 109, 751–762. doi:10.1111/j.1365-2672.2010.04706.x.
- 1151 Zozaya-Valdés, E., Egan, S., and Thomas, T. (2015). A comprehensive analysis of the microbial
1152 communities of healthy and diseased marine macroalgae and the detection of known and
1153 potential bacterial pathogens. *Front. Microbiol.* 6, 146. doi:10.3389/fmicb.2015.00146.
- 1154 Zozaya-Valdés, E., Roth-Schulze, A. J., and Thomas, T. (2016). Effects of temperature stress and
1155 aquarium conditions on the red macroalga *Delisea pulchra* and its associated microbial
1156 community. *Front. Microbiol.* 7, 161. doi:10.3389/fmicb.2016.00161.
- 1157
- 1158

1159 **Figure legends**

1160 **Figure 1.** Experimental design of the study. (A) Workflow of the full experiment over time. (B)
1161 Details of the waterflow circulating within the experimental devices.

1162 **Figure 2.** Multivariate analyses of surface microbiota and surface metabolomes including all
1163 samples of *T. atomaria*, represented according to their sampling time. (A) weighted UniFrac based
1164 NMDS plots showing β -diversity differences of epibacterial communities. (B) PCA score plots
1165 showing differences of surface metabolomes.

1166 **Figure 3.** Weighted UniFrac based NMDS plots showing differences of β -diversity of epibacterial
1167 communities of *T. atomaria* samples collected at a specific sampling time: (A) t_1 , (B) t_2 , and (C) t_3 .

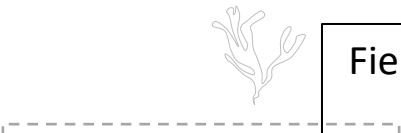
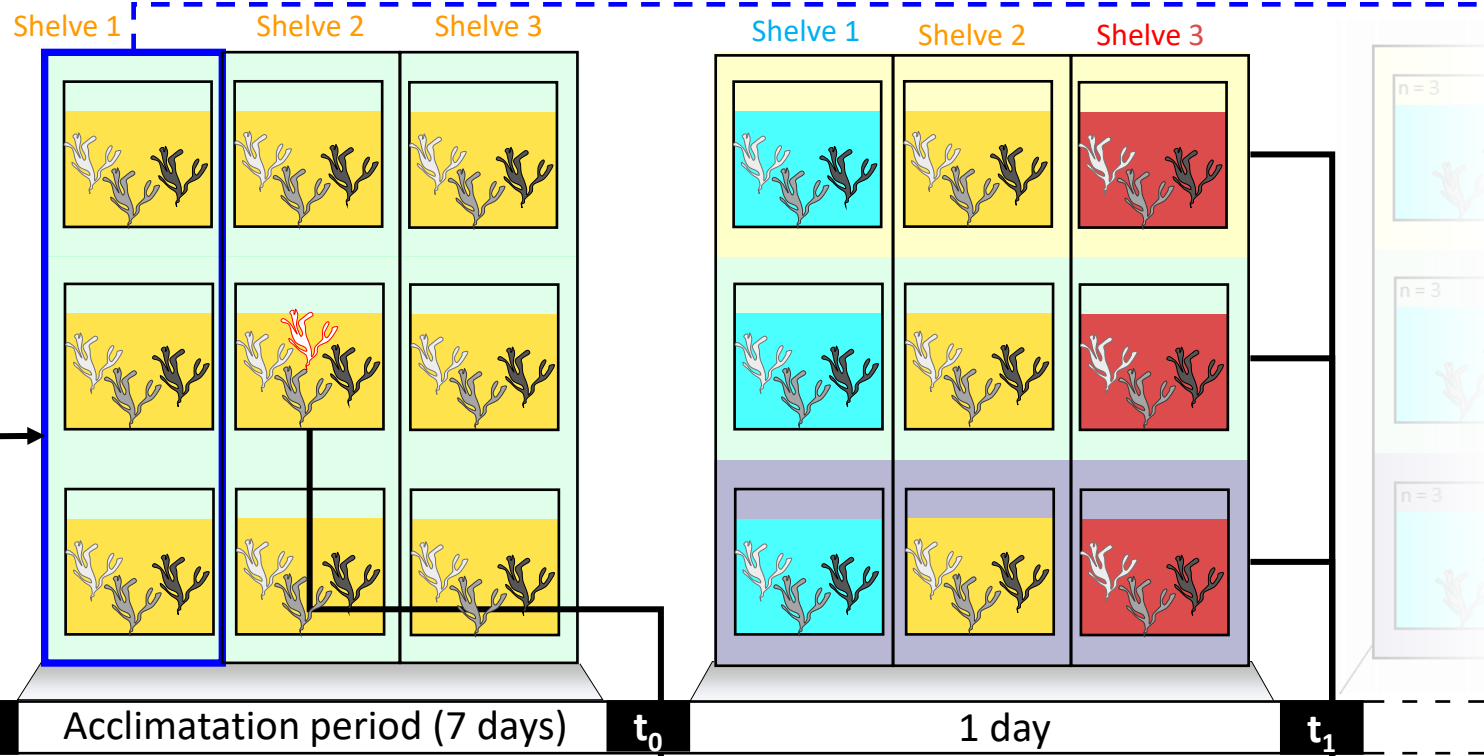
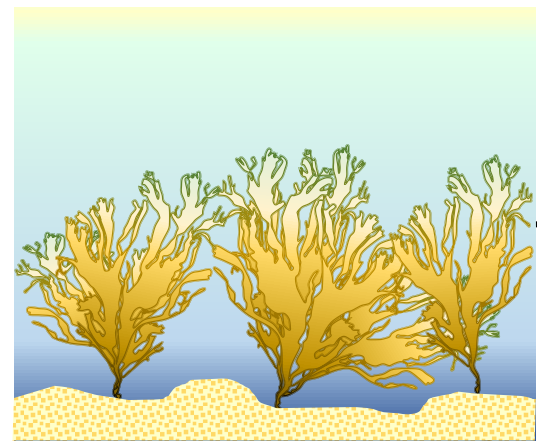
1168 **Figure 4.** Summary of significant variations of discriminant bacterial genera at the surface of *T.*
1169 *atomaria* samples collected at t_3 according to cross-conditions of temperature and irradiance.

1170 An arrow between two aquaria indicates a significant difference of relative abundance of a
1171 discriminant genus (Duncan's test and Benjamini-Hochberg p -value adjustment) between two
1172 conditions. \nearrow and \searrow symbols after a genus name indicate whether a significant increase or
1173 decrease is respectively observed from the condition where the arrow starts to the condition
1174 where the arrow ends.

1175 **Figure 5.** PCA score plots showing differences of surface metabolomes of *T. atomaria* depending
1176 on the sampling time: (A) t_1 samples, (B) t_2 samples, and (C) t_3 samples.

1177 **Figure 6.** Summary of significant variations of discriminant surface metabolites of *T. atomaria*
1178 according to cross-conditions of temperature and irradiance at t_3 .

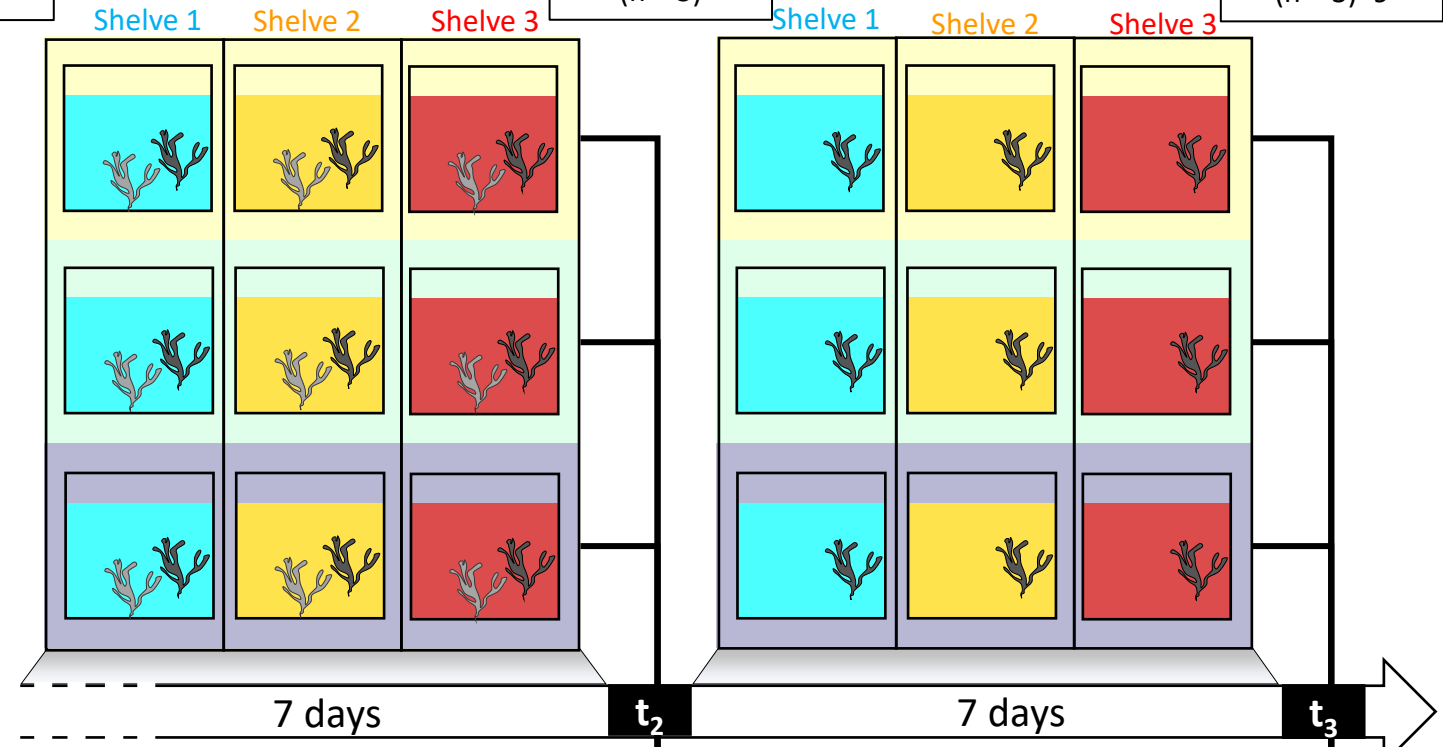
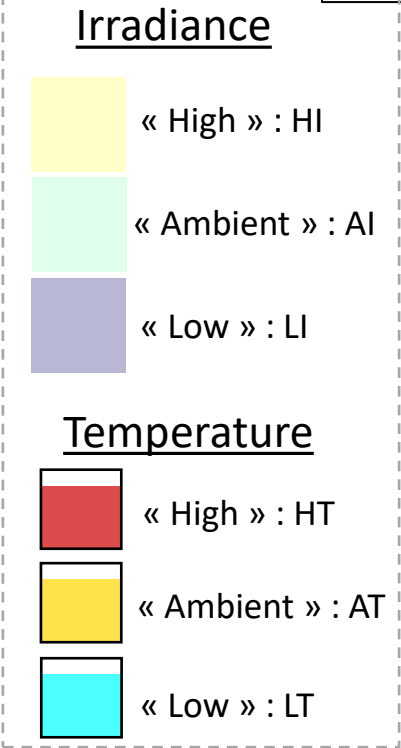
1179 An arrow between two aquaria indicates a significant difference of the normalized concentrations
1180 of a chemical biomarker (ANOVA and Tukey's tests) between two conditions. \nearrow and \searrow symbols
1181 after a compound name indicate whether a significant increase and decrease is respectively
1182 observed, from the condition where the arrow starts to the condition where the arrow ends.

A

Field samples (n = 3)

t_0 samples (n = 3)

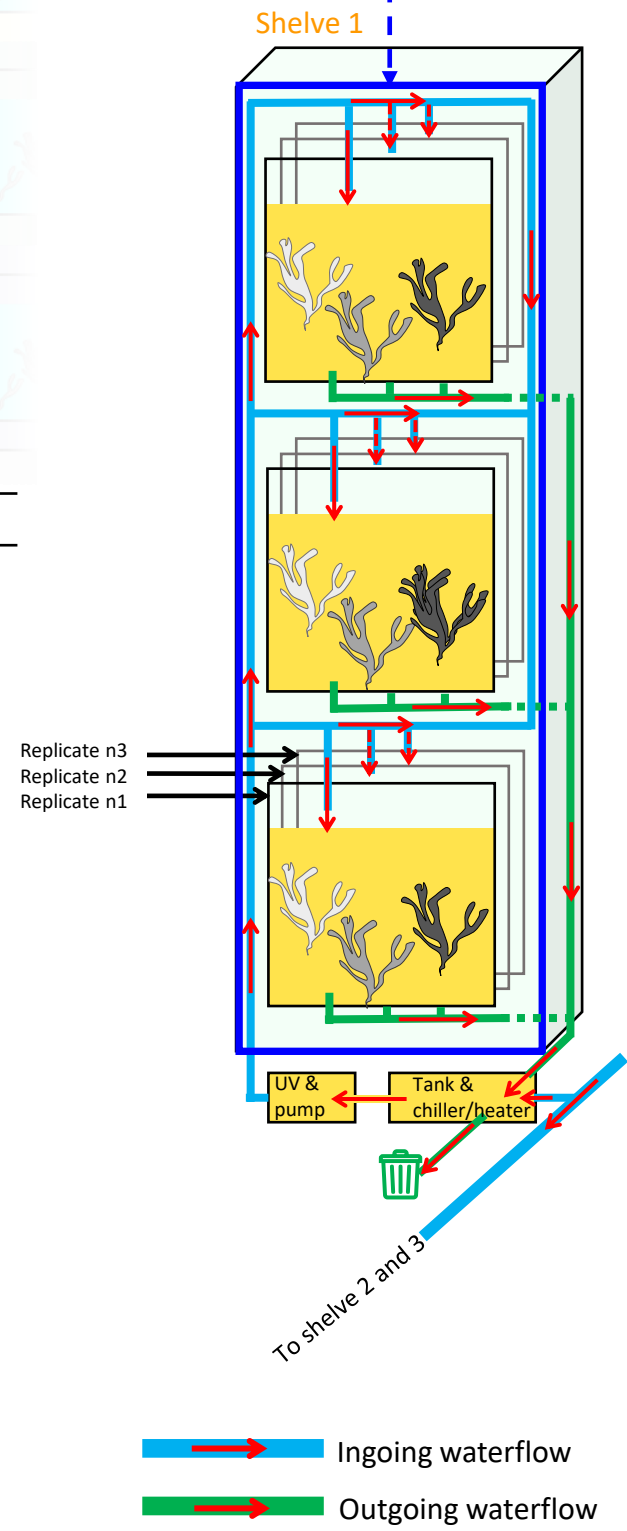
t_1 samples (n = 3)*9

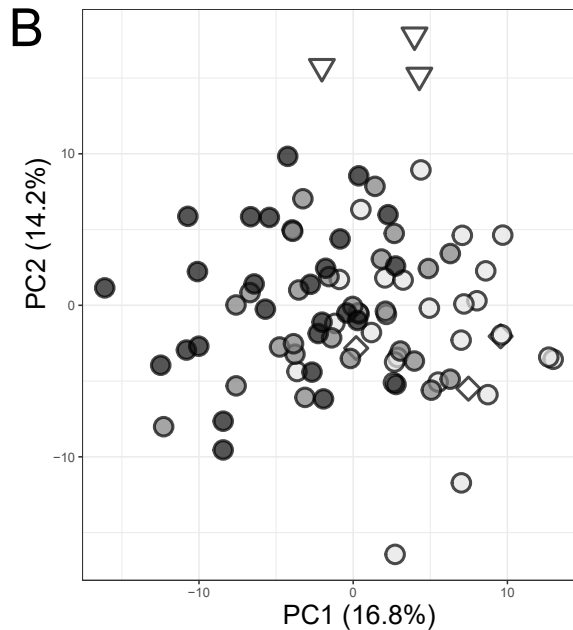
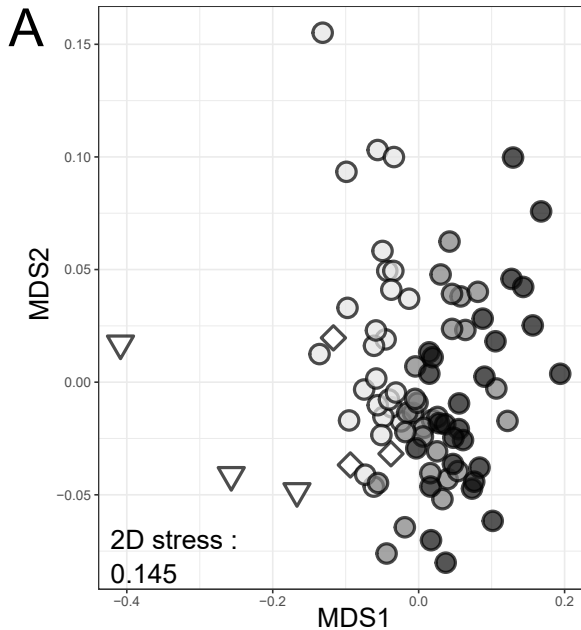


7 days

t_2 samples (n = 3)*9

t_3 samples (n = 3)*9

B



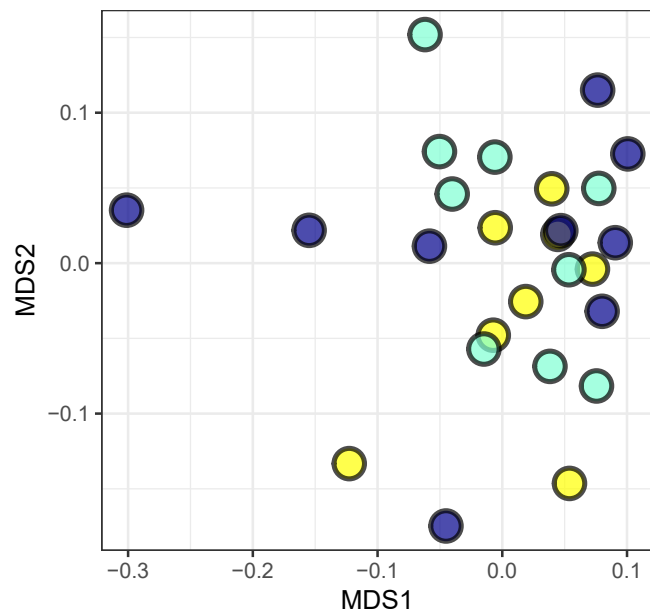
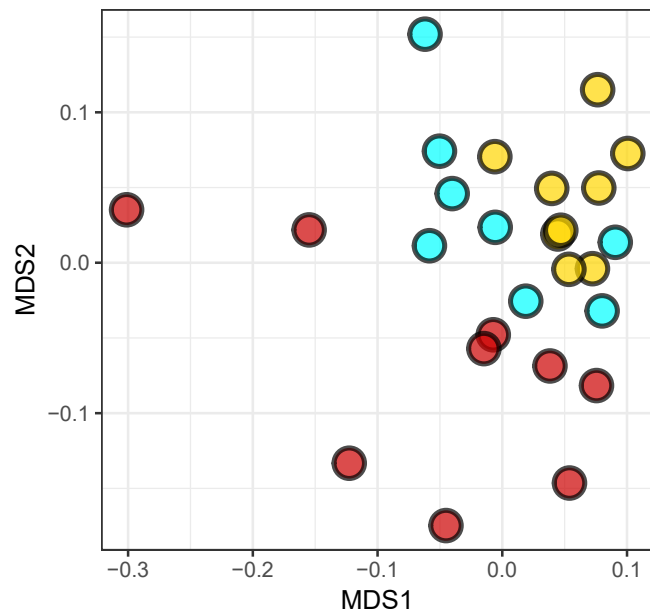
▽ "Field" samples

◇ "Acclimated" samples (t_0)

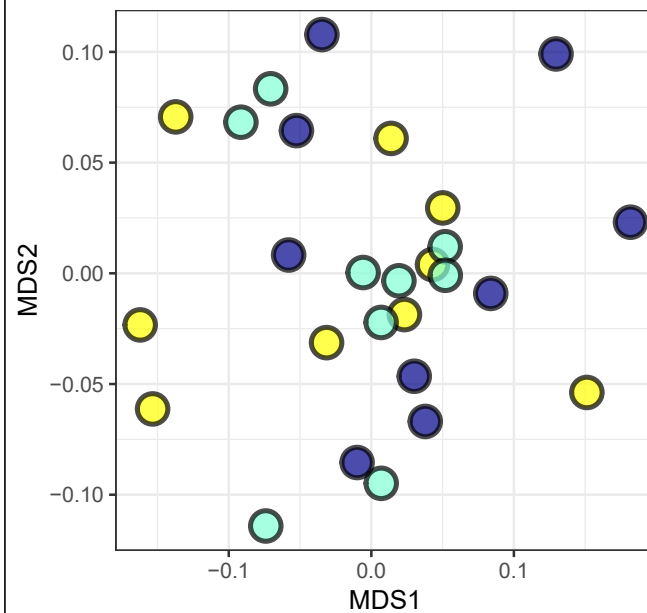
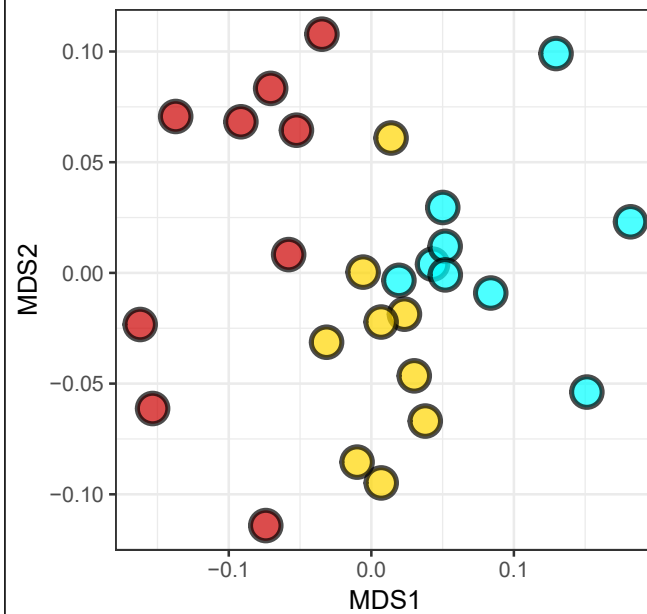
○ t_1 ($t_0 + 24$ hours) samples

● t_2 ($t_0 + 7$ days) samples

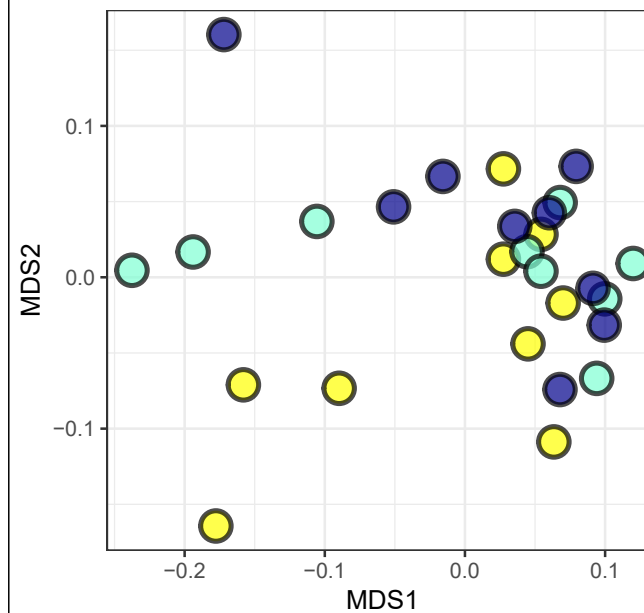
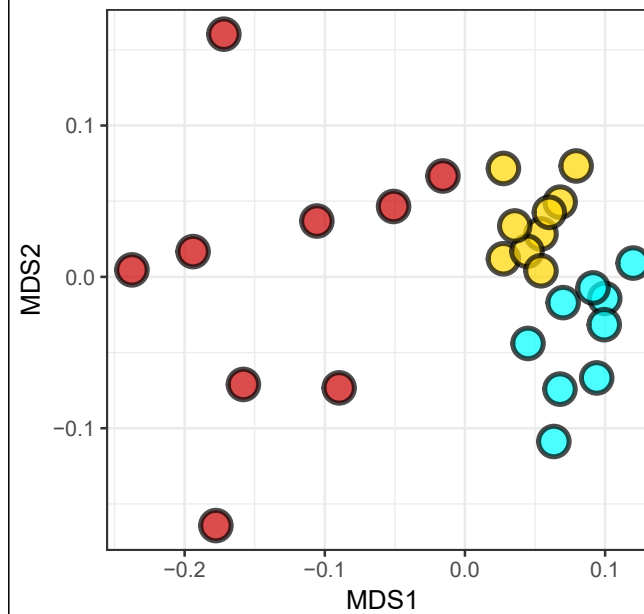
● t_3 ($t_0 + 14$ days) samples

At₁ (to + 24 hours)

2D stress = 0.169

Bt₂ (to + 7 days)

2D stress = 0.177

Ct₃ (to + 14 days)

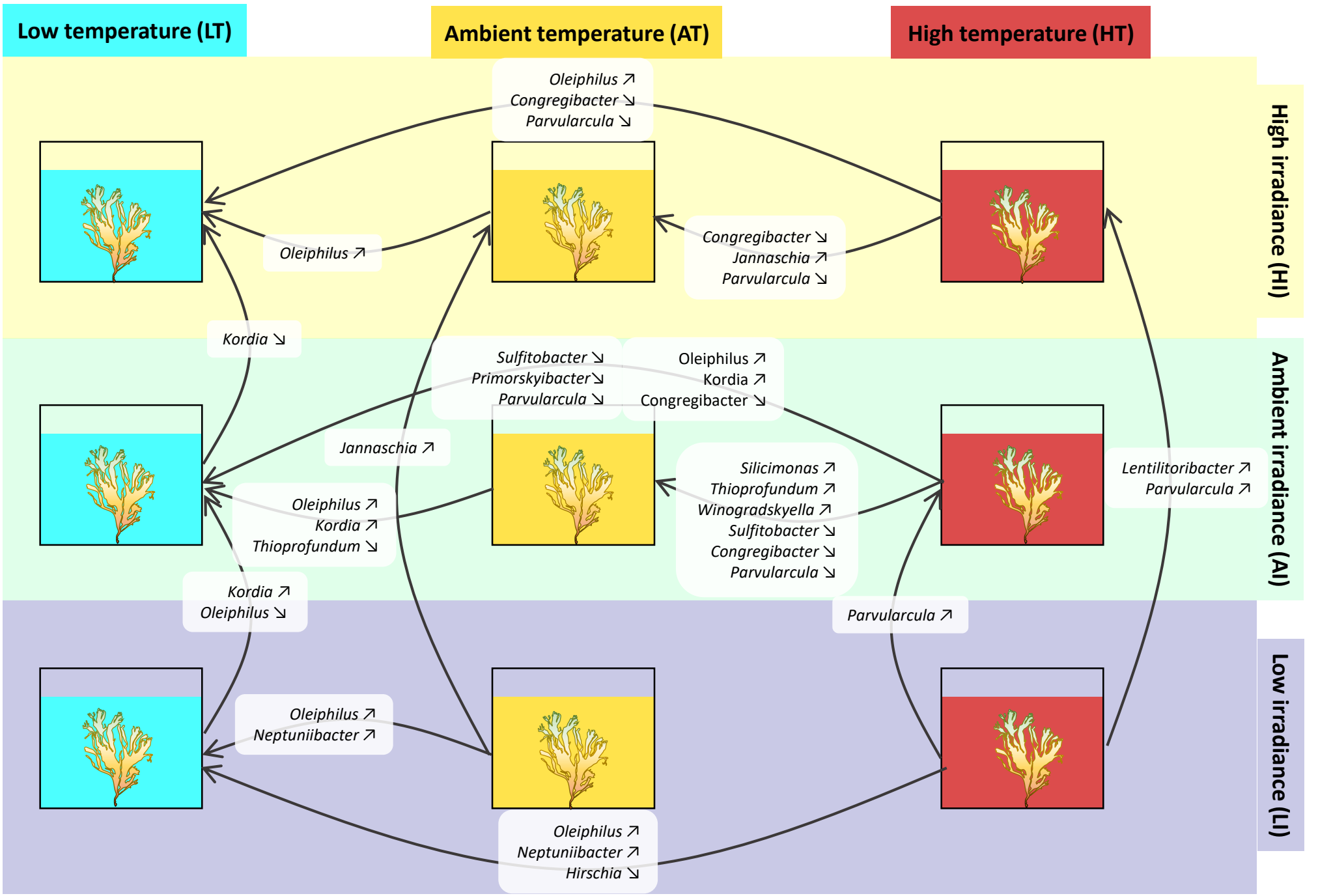
2D stress = 0.146

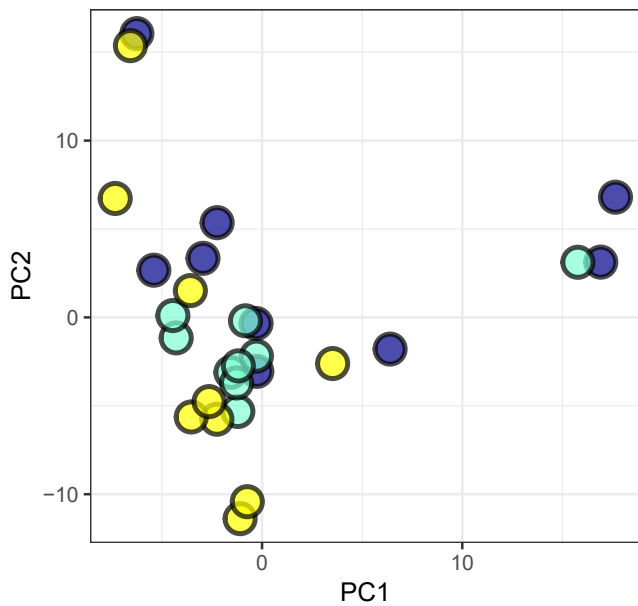
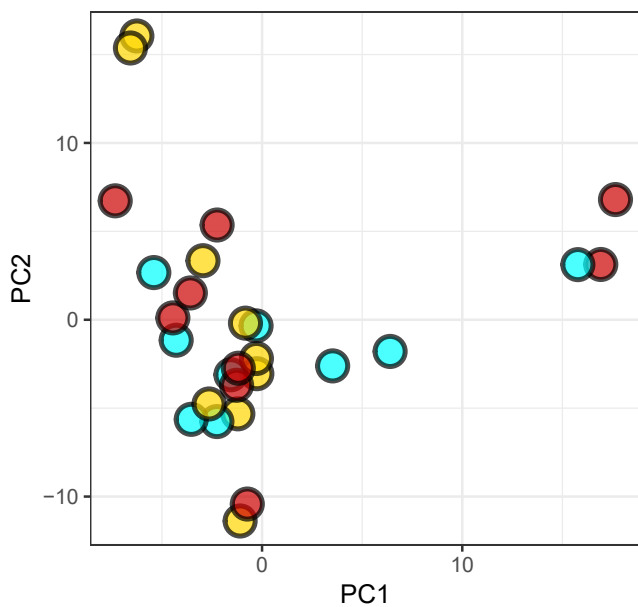
Temperature

- "High" : HT
- "Ambient" : AT
- "Low" : LT

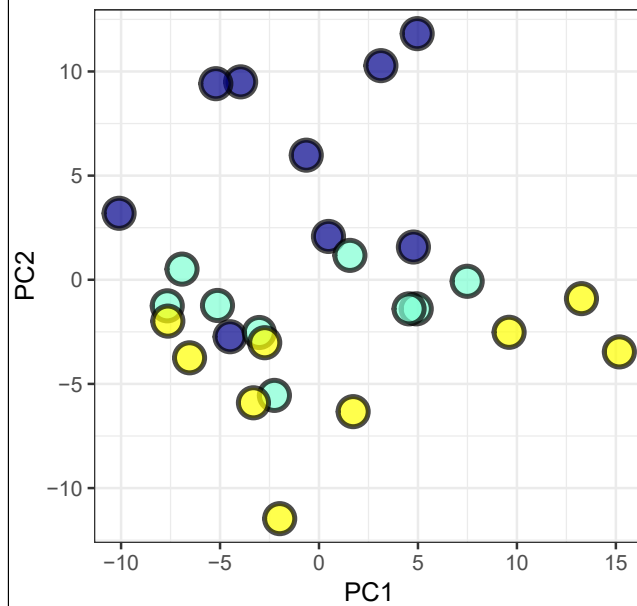
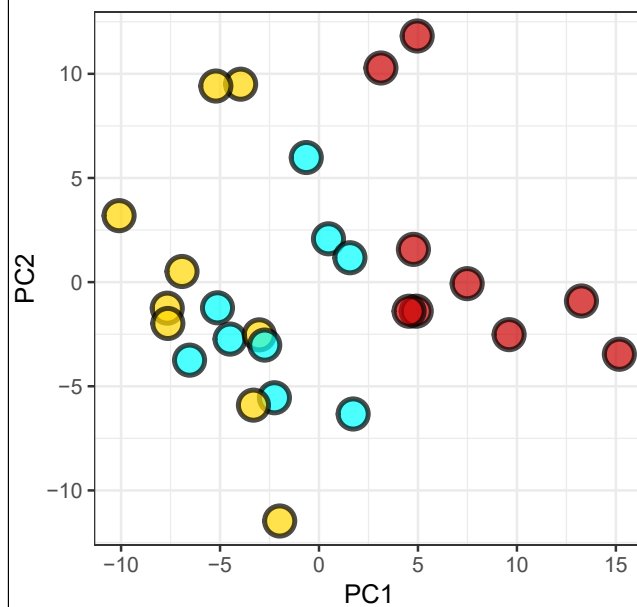
Irradiance

- "High" : HI
- "Ambient" : AI
- "Low" : LI

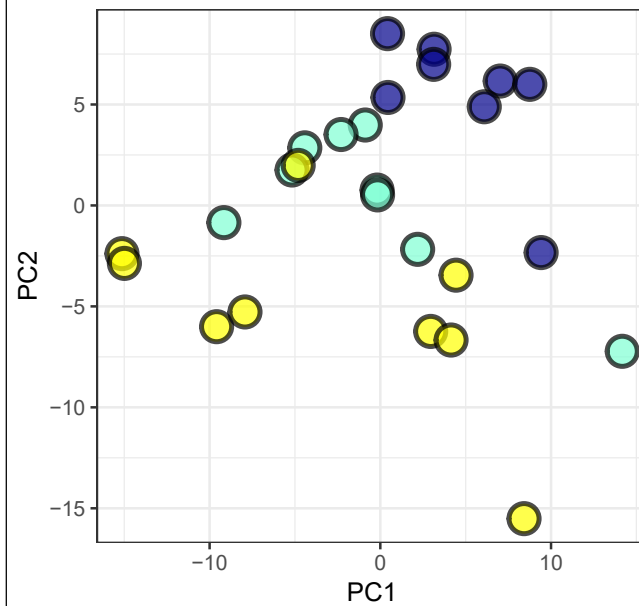
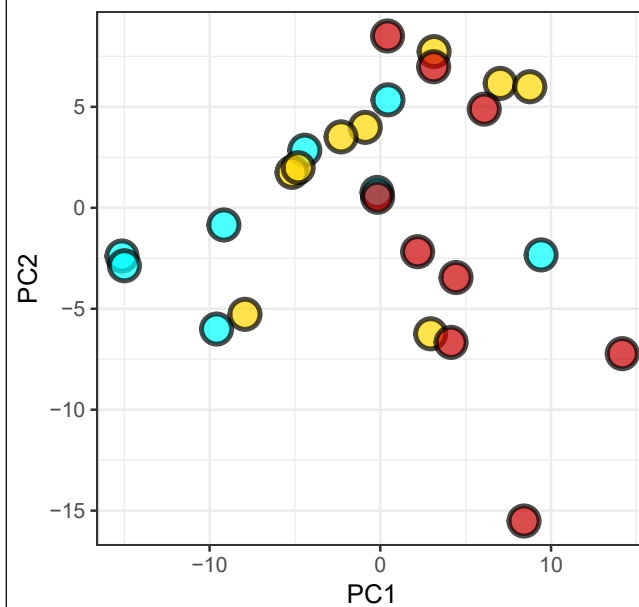


A t_1 ($t_0 + 24$ hours)

PC1 : 23.4 % ; PC2 : 21.3 %

B t_2 ($t_0 + 7$ days)

PC1 : 24.5 % ; PC2 : 16.2 %

C t_3 ($t_0 + 14$ days)

PC1 : 24.8 % ; PC2 : 14.4 %

Temperature

"High" : HT

"Ambient" : AT

"Low" : LT

Irradiance

"High" : HI

"Ambient" : AI

"Low" : LI

Low temperature (LT)

Ambient temperature (AT)

High temperature (HT)

High irradiance (HI)

Ambient irradiance (AI)

Low irradiance (LI)

